Investigation of Wind Variability in the South Atlantic Sector of the Southern Ocean and the Influence on the Upper Ocean in a Numerical Ocean Model

Supervisor: A/Prof. Marcello
Co-supervisors: Dr. Nicolette Chang and Dr. Sarah Nicholson

University of Cape Town

Department of Oceanography

Tumelo Comfort Moalusi

Supervisor: A/Prof. Marcello

Co-supervisors: Dr. Nicolette Chang and Dr. Sarah Nicholson

Acknowledgements

Dr. N. Chang, S. Nicholson and A/Prof. M. Vichi have been ideal supervisors. Their sage advice, humorous criticisms, and patient encouragement supported the writing of this thesis in many ways. I would also like to express my gratitude to the Council for Scientific and Industrial Research for financial support provided. I am also thankful to the Centre for High Performance Computing (CHPC) for the computational hours provided for this analysis.

List of Figures

List of Tables

Acronyms

AABW - Antarctic Bottom Water
AAIW - Antarctic Intermediate Water
ACC - Antarctic Circumpolar Current
AZ - Antarctic Zone
CDW - Circumpolar Deep Water
CO_2 - Carbon Dioxide
ECMWF - European Centre for Medium-range Weather Forecasts
EKE - Eddy Kinetic Energy
ENSO - El Niño Southern Oscillation
EOF - Empirical Orthogonal Functions
MLD - Mixed Layer depth
MSLP - mean sea level pressure
NCEP - National Centers for Environmental Prediction
NEMO - Nucleus for European Modelling of the Ocean
SAO - Semiannual Oscillation
SH - Southern Hemisphere
SAM - Southern Annular Mode
SAMI - Southern Annular Mode index
SAF - Subantarctic Front
SAMW - Subantarctic Mode Water
SAZ - Subantarctic Zone
SO - Southern Ocean
SSH - Sea Surface Height
SST - Sea Surface Temperature
SSS - Sea Surface Salinity
STF - Subtropical Front
STZ - Subtropical Zone
PC - Principal Component
PF - Polar Front
WOA - World Ocean Atlas

Table of contents

Abstract

Several papers have linked climate variability in the Southern Ocean (SO) with the Southern Annular Mode (SAM), which has seen an increase in the positive phase since the mid-1960s, due to the Antarctic ozone depletion and emissions of greenhouse gases. The SAM is recognized as the main mode of atmospheric variability in the SO. The SAM index allows an understanding of the latitudinal movement (south-north) of the westerly wind belt circling Antarctica and has significant impacts on Antarctic surface temperatures, ocean circulation, and many other aspects of Southern Hemisphere climate and thus the global ocean. During negative phases of the SAM Index, westerlies intensify and move north, bringing about more (or stronger) storms, and low pressure systems over southern Australia.

The changes associated with SAM forcing may have impacts on carbon uptake and storage in the SO directly through upwelling and outgassing, and indirectly, by influencing nutrient cycles and phytoplankton activity. Understanding the variability of the wind field in the SO and how it affects ocean circulation, climatic and oceanic variables is important. Thus, this thesis presents the relationship of the SAM index and the upper ocean, specifically analysing sea surface salinity (SSS), sea surface temperature (SST) and the mixed layer depth (MLD), in the Southern Atlantic sector of the SO as presented in numerical ocean models. Two resolutions of NEMO ocean model are compared: a) eddy-permitting (SATLANTIC05), b) eddy-resolving (SATLANTIC12) models, with horizontal resolutions of ½ and 1/12 °, respectively. In situ data from 2013 World Ocean Atlas is used as a benchmark for the analysis.

Our model-based analysis confirms previous studies done on the influence of the SAM on the SO, that a strong relationship exists. The SAM index is positively correlated with wind speed in the Antarctic Zone (AZ) and negatively correlated in the Subantarctic Zone (SAZ). The impacts of this is clear in the upper ocean. These correlations between SAM index and the selected variables at these selected locations confirms that the SAM index corresponds with cool surface temperatures at higher latitudes and a weak cooling at midlatitudes during positive phase, which differs regionally.

1. Introduction

The Southern Ocean (SO) contribute significantly to the world's global climate. SO is home to the most vigorous large-scale ocean and atmospheric circulation in the global ocean: The Antarctic circumpolar trough and associated westerly wind belt drives the underlying ocean (Rintoul et al. 2018). This air-sea circulation in turn contributes to the global transportation of important climate quantities such as, heat, fresh water, nutrients and anthropogenic CO_2. These quantities are then transferred from the surface to the deep sea when Subantarctic Mode Water (SAMW) form (Lovenduski and Gruber et al. 2005; Rintoul et al. 2001; Sarmiento et al. 2004). SAMW form when mixed layers deepen during winter convection, and the resulting mixing occurring in mixed layers towards northern Subantarctic Front (SAF) in the Southern Hemisphere (Hartin et al. 2011). SAMW form in deep winter mixed layers where nutrient-rich waters south of the Polar Front (PF) and the low nutrient waters north of the Subtropical Front (STF) mix (Rintoul and Trull et al. 2001). SAMW form when winter mixing extends to greater depths in the SAZ. Nearly 40% of the annual oceanic uptake of anthropogenic carbon dioxide from the atmosphere has been accounted for by the area south of 30 °S, making the SO one of the primary determinants of global oceanic CO_2 uptake (Russel et al. 2018).

Several papers have linked oceanographic and atmospheric changes in the SO with the dominant mode of climatic variability, known as the Southern Annular Mode (SAM, Marshall et al. 2003; Thompson and Solomon et al. 2007; Thompson and Wallace et al. 2000). The SAM explains over 20% of atmospheric pressure variations in the Southern Hemisphere (Thompson and Wallace et al. 2000), and thus contributes to SH climate variability from low to high frequency time scales (a few days to decades) (Fogt et al. 2012; Kidson et al. 1999). The SAM gives an understanding of the latitudinal movement (South-North) of the westerly wind belt circling Antarctica (Gong and Wang et al. 1999; Thompson et al. 2000). Its influence is clear in a number of variables both in the ocean (sea surface temperature (SST), sea surface salinity (SSS), etc.) and atmosphere (surface air temperature and sea-level pressure).

The characteristic patterns of the predominant atmospheric circulation over Antarctica are indicated by the SAM index, which has seen an increase towards the positive phase over the past few decades. The shift is believed to be linked with the Antarctic ozone depletion and emissions of greenhouse gases (Gong and Wang et al. 1999; Thompson et al. 2000). The SAM is fully described later in Section 1.4.

Positive values of the SAM index, that is, when SAM is in its positive phase, are associated with the contraction of the westerly wind belt, bringing about relatively lower pressure anomalies over Antarctica compared to those in the mid-latitudes, which significantly strengthens westerlies at ~55 °S (Lovenduski and Gruber et al. 2005; Thompson and Wallace et al. 2000; Fyfe et al. 2003). Conversely, during the negative phase of SAM, the westerly wind belt expands and moves towards the equator, yielding an increased presence of low pressure systems in the around Antarctica (Thompson and Solomon et al. 2007; Gillet et al. 2006).

Many recent modelling studies have shown that the resulting wind-driven responses during a positive phase of the SAM, induces an increase in both the vertical tilt of isopycnals which induces a more intense Antarctic Circumpolar Current (ACC, Hall and Visbeck 2002; Yang et al. 2008; Farneti et al. 2010) and a minor southward shift, in the order of a few degrees (Spence et al. 2010).

Ocean models are important tools used to numerically represent large space-time scales that give an understanding of the ocean climate system (GriÅes et al. 2000). Due to Inabilities to handle oceanic controlled experiments on large scale climate systems, the use of ocean models has increased over the past decades. Biases between model outputs, in situ observations and the same characteristics observed from satellites in space are highly reduced, largely due to the steady growth in computer power and ever growing volumes of available data. This suggests that the quality of results drawn from ocean models is well trusted within the climate science community (Griffies et al. 2004).

In this thesis, the effect of the wind field properties in the South Atlantic sector of the SO and its effect on the underlying ocean are investigated in an ocean model at two different horizontal resolutions. More specifically, the focus is on the impacts of the dominant mode of atmospheric variability in the SO, SAM, on temperature, salinity and mixed layer depth (MLD) and its link to the numerical spatial scales. Understanding how variability of the wind field in the SO affects key variables of the ocean circulation can help in improving our understanding of future global changes.

1.1. About the Southern Ocean

The SO is home to the world's only global current, the Antarctic Circumpolar Current (ACC). The strong eastward flowing current is often called the "great ocean conveyor" because it connects the three major ocean basins: Atlantic, Indian and Pacific Oceans due to the lack of any interrupting landmass. The ACC transports significant climatic quantities such as heat, fresh water and nutrients around the globe (Lovenduski and Gruber 2005; Schmittner et al. 2007). The ACC enhances upwelling of deeper waters and helps regulating carbon dioxide (CO_2) exchange between the deep sea and the atmosphere. These large (and small) scale processes contribute to making the SO a major influencer of global climate (Anderson et al. 2009).

SO overturning circulation is made up of two cells (Figure 1). Circumpolar Deep Water (CDW) result from mixing of all the World's oceans (Dinniman et al. 2012). The relatively salty, warm current (up to 3.5 °C above freezing point), low density water mass, spreads poleward and shoals, and ultimately outcrops at the sea surface within the ACC belt. The CDW flows onto the continental shelf at depths of more than 300 m, upwells south of the ACC, where interactions with sea ice and atmosphere convert the upwelled water to a denser water mass known as the Antarctic Bottom Water (AABW). Forming the lower cell of the overturning circulation. At the sea surface, a relatively light water mass: upper CDW (UCDW) outcrops within the ACC belt, where it is driven towards the equator in the Ekman layer and converted to less dense intermediate water, by heat and freshwater build up from the atmosphere. By so doing, forming the upper cell (Rintoul et al. 2013).

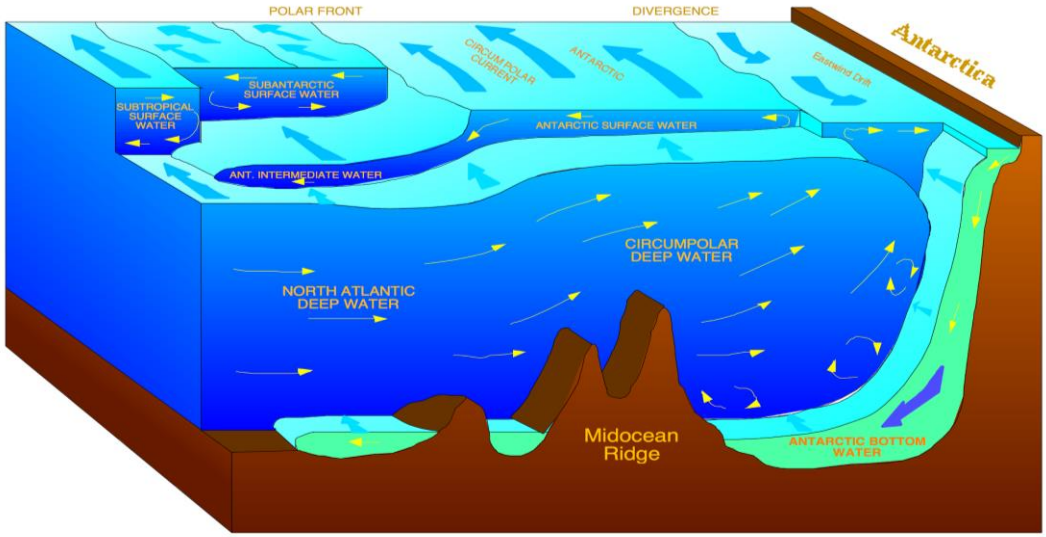

Figure 1: A schematic view of circulation in the SO. The yellow lines indicate overturning circulation. The eastward flow of the ACC. (From Antarctic Glaciers website). The heavy yellow arrow and dashed yellow lines denote the eastward flow of the ACC. The overturning circulation is shown by dark arrows, and the wavy arrows are intended to represent transport by eddies (from Rintoul et al. 2013).

1.2. Fronts and zones in the Southern Ocean

Fronts in the ocean are regions in which properties change significantly over short distances. The distance depends on the degree/scale of the process forming the front and may only be a few meters wide south to north. It is worth noting that changes in some of the properties defining fronts i.e. temperature and salinity, are in magnitude larger than those on either side of the fronts, with the same properties, over the same distance. The fronts, therefore, help us define regions of constant oceanography in the SO.

There are three main large-scale fronts in the SO: the STF, the SAF and lastly the PF, (Figure 2). Regions between fronts, where properties are more uniform, are referred to as zones. The SAZ located between the STF and the SAF, marks the boundary between warm, salty tropical waters and colder subantarctic waters.

The SAF is located around 50 - 51 °S. The PF is located a few degrees (4-5°) south of SAF and is characterized with minimum temperature waters at 2 °C at 200 m depth, although slightly cooler waters extends near 52.5 °S. South of the PF is the AZ, a region with fairly homogenous surface properties characterized by a low concentrations of salinity (33.9 psu) due to sea ice melting and the near surface temperature minimum layer of ‘‘Winter Water” (Chaigneau et al. 2002). The PF and SAF are responsible for the majority of the ACC zonal transport.

The zone poleward of the PF is known as the AZ, a region that is seasonally covered by a large expanse of sea ice. This area is known for the high productivity which accounts for widespread phytoplankton blooms in spring-summer (Arrigo et al. 2008b). The AZ is also known for the dramatic meridional gradients in mixed layer, salinity and temperature (Manucharyan and Thompson et al. 2017).

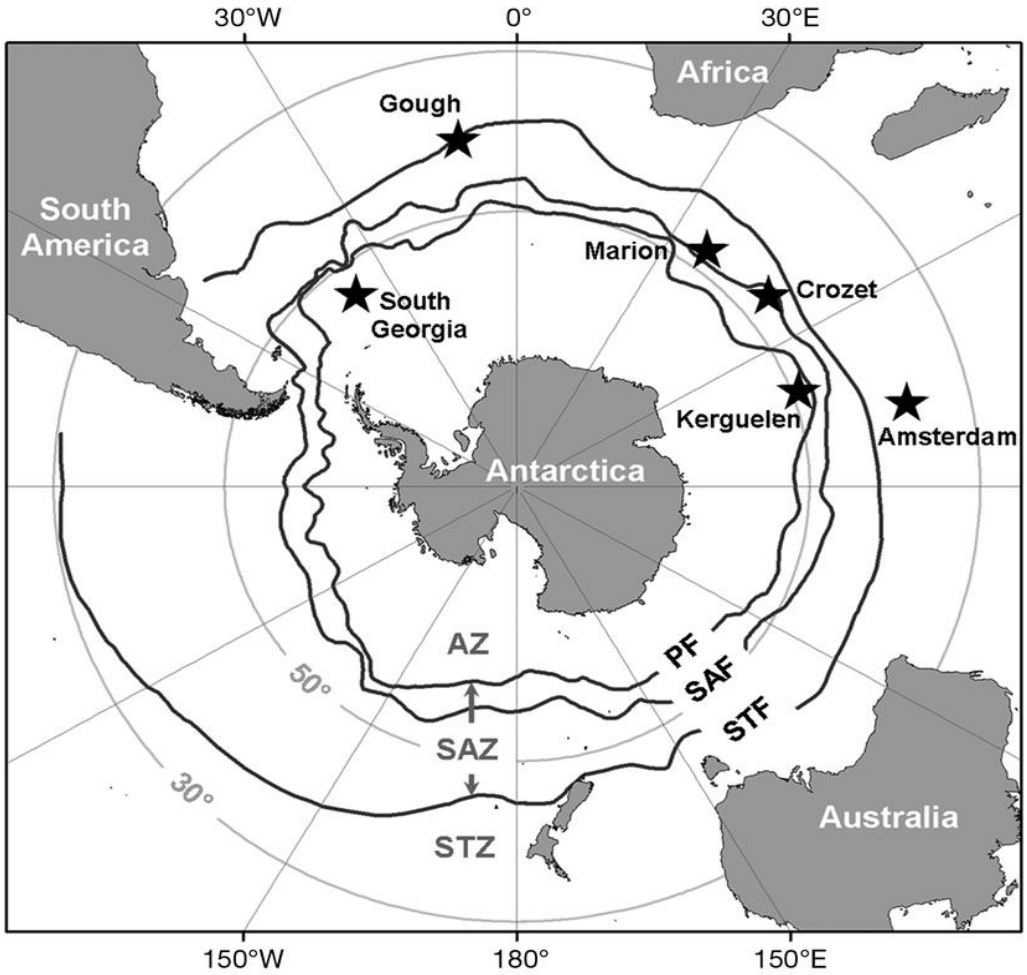

Figure 2: The surface regime of the SO showing the 3 main fronts, zones and the main topographic features in the open ocean (Jaeger et al. 2013 based on Orsi et al. 1995).

1.3. Atmospheric variability on the Southern Ocean

There are a few important modes of atmospheric variability in SH, such as El Niño Southern Oscillation (ENSO), Southern Annular Mode (SAM) and the Semi-annual Oscillation (SAO). This work focuses on the role of the SAM index on ocean variables, and the other modes are briefly summarized. The SAO results from differences in the annual cycles of temperature over the Antarctic continent and the mid-latitude oceans. This has an influence on the meridional temperature gradient (baroclinicity) at high latitudes. There are many effects and implications as a result of SAO on the physical and biogeochemical processes in the SO. Inducing responses in, among others, mean winds, cyclone characteristics, surface currents, Ekman drift and sea ice distribution (Simmonds, et al. 2003; Watkins and Simmonds et al. 1999).

ENSO refers to the ocean-atmosphere exchange in the tropical Pacific that results in a seasonal variation between lower-normal and higher-normal (or an anomalous) SSTs and dry and wet conditions over the course of a few years. During an El Niño, sea level pressure tends to be lower in the eastern Pacific and higher in the western Pacific while the opposite tends to occur during a La Niña. This see-saw in atmospheric pressure between the eastern and western tropical Pacific is called the Southern Oscillation, often abbreviated as simply the SO. The link between the two Southern Oscillations: SAM and ENSO is considered strong, in fact the negative phase of the ENSO contributes to the positive phase of the SAM (Gong and Wang et al. 1999).

1.4. The Southern Annular Mode (SAM)

Several modes of climate variability in the SO have been introduced above. However, this thesis focuses on the mode of atmospheric variability dominating the Southern Hemisphere, the Southern Annular Mode (Thompson and Solomon et al. 2007). Several papers have used different names for it: high-latitude mode (Rogers and van Loon et al. 1982), the Antarctic Oscillation (Gong and Wang et al. 1999) and the southern annular mode (SAM) (Limpasuvan and Hartmann et al. 1999). It shall be referred to as the Southern Annular Mode (SAM) throughout this thesis. It is termed “annular” as it has a nearly uniform zonal pattern across the high Southern latitudes in its mean state (Fogt et al. 2011). SAM gives an understanding of the South-North movement of westerly wind belt circling Antarctica and thus influences atmospheric variability in the SO up to the equator (Marshall et al. 2003).

Different definitions of SAM indices include Principal Component (PC) analysis which uses the first PC of a Southern Hemisphere extratropical climate variable, e.g. geopotential height,

mean sea level pressure (MSLP) or temperature (e.g. Thompson and Wallace, 2000; Nan and Li, 2003) and the Gong and Wang (1999) method, which calculates the difference between normalised zonal MSLP between 40° S and 65° S as shown in Eq. (1) below:

$$Gong\ \&\ Wang\ =\ P^{*}\quad 40^{\circ}S\ -\ P^{*}\quad 65^{\circ}S \qquad (1)$$

Where: P^{*} is the monthly normalized zonal MSLP (at 40 °S and 65 °S). SAM indices differ in either the climate variables used, the data sources used, the method used to define the index, or the time period over which they are determined (Ho et al. 2012).

Several authors (Kidson et al.1999; Gong and Wang et al. 1999; Marshall et al. 2003) have defined the SAM index using methods mentioned, all of which give the same general result: positive increase in the SAM index since the 1950s. Kidson (1999) used the third Empirical Orthogonal Functions (EOF) in a 300-hPa stream function NNR data mean run over 11 months from 1957. Gong and Wang (1999) calculated the SAM using NNR MSLP data from an identical period. Marshall (2003) used the same definition as Gong and Wang (1999) to calculate the SAM index, but using observed pressure differences between six stations close to 40 °S and six stations close to 65 °S. Marshall's SAM index was developed as an alternative to re-analyses-based indices, which are of questionable quality before ~1979. The index is available from 1957 to the present and is available here. Figure 3 shows the seasonal values of the observation-based SAM index.

The SAM index, defined by the leading principal component of the 700 mb geopotential height anomaly south of 20 °S in the atmosphere, has been experiencing a shift towards the positive phase since the mid-1960s, one notable "extreme" negative event was in 1964 just before this positive trend, it is believed that it was caused by the Agung eruption from the previous year. The eruption had a greater negative effect on tropospheric temperatures in the southern mid-latitude than it had on the high latitudes. (Marshall et al. 2011; Angell et al 1988 and Lovenduski, and Gruber et al. 2005), however the greatest changes occurred in the late 1970s.

During the 1990s, the SAM index was mainly positive with stronger events occurring during 1993–1994 and 1998–2000. After 2000, the index has been oscillating around zero, with a few negative events occurring during 2000–2001, 2002 and later in 2012 and a year later in 2014. These inter-annual changes in the strength of the SAM may also modify the strength of atmospheric convergence and divergence in the different years, leading to inter-annual variations in sea level (Morrow et al. 2006). Model simulations also suggest that this positive trend is due to greenhouse gases and aerosols (Fyfe et al. 1999). Figure 3 below shows the

signature of the station-based SAM index by Marshall et al. (2003) used in this thesis, which extends back to 1957, provided by Trenberth et al. (2007, last modified 19 March 2018).

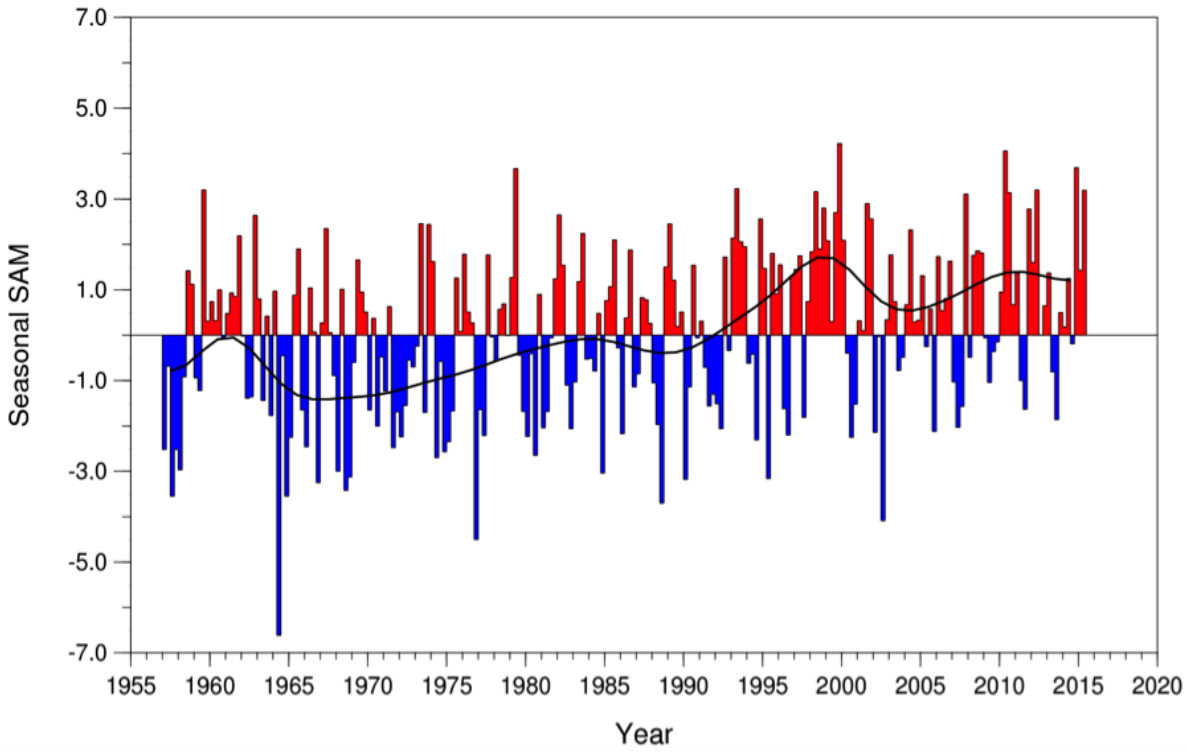

Figure 3: Seasonal values of the observation-based SAM index (Marshall et al. 2013). The smooth black curve shows decadal variations.

1.4. Response of the SO to SAM

The ocean responds differently to different modes of variability. In the Eastern Pacific, for instance, during an El Niño event of ENSO, the sea temperature warms, while it cools during a La Niña. During positive SAM, westerly winds are enhanced over the AZ and PFZ, bringing about increases in the Ekman transport towards equator and cold sea surface temperature anomalies in these regions. The positive phase of the SAM is also associated with easterly wind and warm SST anomalies in the Subtropical Zone (STZ), and increased convergence of water, resulting in an increase in downwelling in the SAZ (Lovenduski, and Gruber et al. 2005). Conversely, during a negative SAM, the westerly wind belt expands towards the equator, which results in more low pressure systems and heavier storms and wet conditions over the south-western Africa (Thompson and Solomon et al. 2007). Some of these characteristics are shown in Figures 4 and 5 below.

The response of the SO to SAM has been widely studied, but due to lack of long-term observational data, studies focusing on the mixed layer or the interior structure of the ocean were drawn from models (Sallée et al. 2010; Hall and Visbeck et al. 2002). Although response of some oceanic variables to SAM appear zonally symmetric in the SO, frontal responses are not, resulting in different frontal features (Sallée et al. 2010). For example, the increase of westerlies around the PF suggests a northward Ekman transport anomaly, while an increase in easterlies at SAF creates a poleward transport anomaly, which results in Ekman convergence at the SAZ and increased downwelling at SAF. The divergence created at the AZ intensifies upwelling near Antarctica (Sen Gupta and England et al. 2006). The waters southward of the PF are known to experience a significant decrease in SST and increase in chlorophyll during the positive phase of SAM and the opposite in the waters north of the STF (Figure 5, Lovenduski and Gruber et al. 2005).

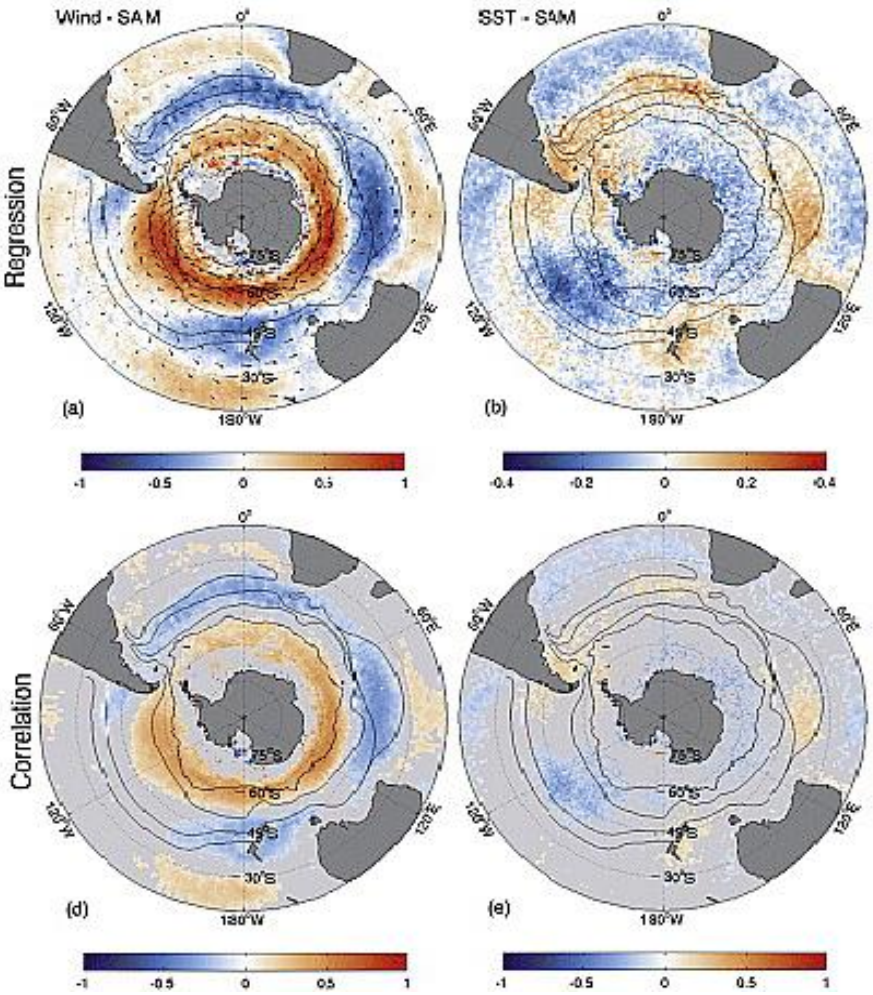

Figure 4: Maps of (a–b) regressions and (d & e) correlations between the SAM index and wind speed and direction and SST, (a & d) and (b & e) respectively from Lovenduski and Gruber (2005). The regression coefficients indicate changes in the wind speed (ms−1), SST (°C). Only those correlation coefficients with significance ≥95% are shown. Black contours mark the location of the SO fronts. From pole to equator these fronts are: Antarctic Polar Front [Moore et al., 1999], SAF, South STF, and North STF [Belkin and Gordon (1996)].

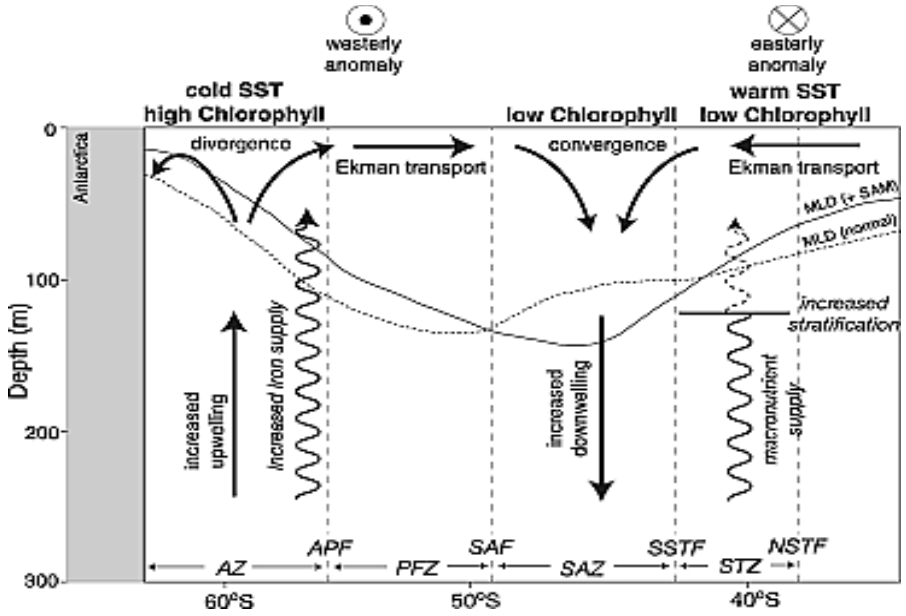

Figure 5: Schematic illustration as shown by Lovenduski and Gruber (2005), of the upper ocean response to a positive phase of the SAM.

The changes associated with SAM forcing may have impacts on carbon uptake and storage in the SO, both directly, through upwelling and outgassing, and indirectly, by influencing nutrient cycles and phytoplankton activity. Moreover, changes in the mixed-layer depth (MLD) have significant implications on the physical and biochemical processes. These responses may be associated with other modes of climate variability that confound the effects SAM possess on SO circulation.

The effects of SAM on the Southern Hemisphere, and more specifically, regions South of Australia and New Zealand have been widely reviewed and documented (Sen Gupta and England et al. 2006; Kidston et al. 2009; etc.), however, there are other areas where investigative work is scarce, specifically the eastern Atlantic sector south of South Africa. Here, SAM is known to affect precipitation patterns over the African continent. Owing to a lack of long-term observations in the remote SO. Reason and Rouault (2005) studied the effects of phases of SAM on the precipitation of Western South Africa using composites of National Centers for Environmental Prediction (NCEP) reanalyses. They found that phases of SAM influence winter rainfall over the area. Furthermore, they observed that most dry/wet winters occur during positive/negative SAM over western South Africa.

Other studies have documented the influence SAM has on local wind forcing and the oceanography in SO at large (Lovenduski and Gruber et al. 2005; Thompson and Wallace et

al. 2000), however, the effects of increasing horizontal resolution on this response of SO oceanography to phases of SAM is lacking in the available literature. As one of the primary drivers of wind circulation over the SO, if satellite and ground truthing observations in the SAM index all exhibit increasing wind speeds over the SO, then this would suggest that the increase in the SAM index has a certain effect on wind speeds, and consequently the oceanography over the SO.

1.5 Key questions

The steady and continuous increase in oceanic wind speed in the SO over the last few decades have attracted significant attention from researchers in a variety of fields including oceanography and climatology (Parker and Wendy et al. 2018). Several papers have attempted to quantify and document the variabilities in wind speeds observed in the SO, and more specifically at a regional level, during different phases of the Southern Annular Mode (Lovenduski, and Gruber et al. 2005; Gillett et al. 2006). One of the primary motivations of this work is to gain a better understanding of the coupling between wind speed variability in the SO and the active phase of the SAM using an ocean model. The following key questions arise:

1. How does wind speed variability influence the surface ocean, namely SST, SSS, MLD and frontal location?
2. What is the role of spatial resolution in the transfer of atmospheric variability to the ocean through the modifying effects of oceanic variables by the SAM?

2. Methods

2.1 Model description

2.1.1 Model configuration

the evolution of the ocean, as a geographical fluid, is governed by physical laws such as the conservation of momentum, energy and mass. The partial differential equations that describe these conservation laws on a sphere have no known analytical solutions. As a result, numerical methods are employed to solve them, thus giving rise to modelling systems such as the one employed in this study, the Nucleus for European Modelling of the Ocean (NEMO). NEMO is a framework of ocean-related numerical engines for oceanographic research, operational oceanography, etc., available in various configurations.

In this thesis, the analysis is run using pre-existing simulations of the NEMO model v3.4 with the SATLANTIC configuration representing the South Atlantic region of the SO, which extends from the Drake Passage to east of Marion Island and 30 °S to Antarctica (See Figure 6 below). This configuration consists of OPA ocean model, LIM2 ice and PISCES biogeochemical models run from 1989 to 2008, although this analysis will only look at the ocean output of the last ten years of the simulation. Spin-up of the model to equilibrium took 2 years. A further description of atmospheric boundary conditions are presented in Section 2.1.2 below.

The SATLANTIC grid is subsetted from the family of ORCA grids (Madec and Lombard et al. 1996), which are available in different horizontal resolutions ranging from about 2 ° to 1/12 °. For the purpose of this study, two model configurations are used: mesoscale-permitting (SATLANTIC05) and mesoscale-resolving (SATLANTIC12) model with horizontal resolutions of ½ ° and 1/12 ° at approximately 48 and 8 km resolution at 30 °S, respectively. Mesoscale-permitting models allows the visualisation of mesoscale activities although smaller processes are not necessarily resolved (e.g. figure 7), in contrast to mesoscale-resolving models which provide realistic fields of turbulent statistics of observed structures (such as eddy fluxes of mass and heat) (Malone et al. 2003). Both models have the same 46 vertical “z” levels at constant depths with partial bottom cells, ranging in thickness from approximately 6 m at the surface to 250 m at depth.

Both models have a closed boundary of the Antarctic continent, i.e. three open boundaries. These 3 lateral boundary conditions for SATLANTIC05 and SATLANTIC12 consist of 5-day mean global model output (ORCA) from ORCA05 and ORCA12, respectively. Treatment for river discharges are included in the model configurations. While temperature is allowed to evolve freely, i.e. not restored to climatology, salinity is restored to Levitus monthly climatology as asserted by Madec and NEMO System Team in the NEMO ocean guide: “The SSS restoring term should be viewed as a flux correction on freshwater fluxes to reduce the uncertainties we have on the observed freshwater budget”.

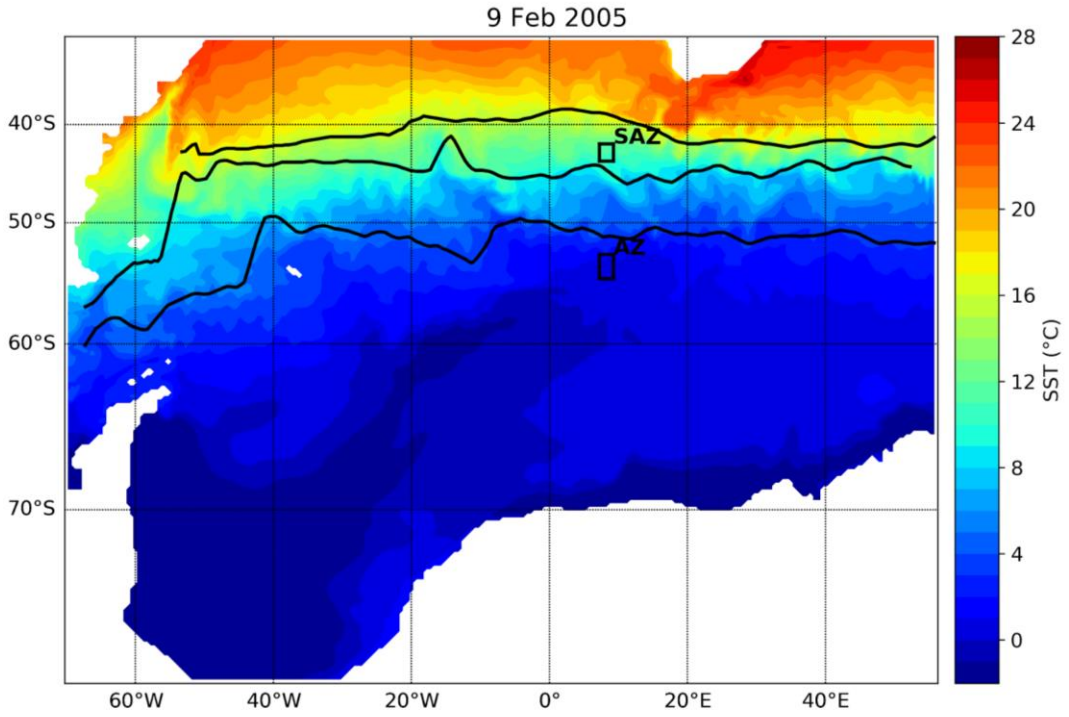

Figure 6: Example of the model output showing the model domain from the SATLANTIC05 model configuration. Also shown, are the fronts: STF, SAF, PF, from north to south and diagnostic boxes representing the SAZ and AZ.

Increasing model resolution helps resolve oceanic processes at a smaller scale. It is therefore crucial to know the threshold at which a specific process is best represented, as increasing resolution might change (improve) the representation of specific process. For example, mesoscale eddies (10 - 100 km) are important for the distribution of surface variables such as SST and SSS, thus the model with the higher resolution is likely to resolve oceanographic processes better.

2.1.2 Atmospheric forcing dataset

The datasets used in this study are ERA-Interim and the World Ocean Atlas 2013 (WOA13). WOA13 (often referred to as "Levitus" or the "Levitus Climatology" after its pioneering creator, Sydney Levitus) is a collection of climatological mean gridded at a horizontal resolution of 1 and ¼ degree. It is based on in situ observations from a number of various sources, providing global, decadal averages of temperature, salinity, oxygen and nutrients at monthly, seasonal and annual intervals for the past six decades (World Ocean Atlas 2013).

ERA-Interim is the 4th generation of climate reanalysis from the European Centre for Medium-range Weather Forecasts (ECMWF, Dee et al. 2011). This is regarded as one of the most reliable reanalyses over the Amundsen and Bellingshausen Seas, and over Antarctica (Purich et al. 2013; Bracegirdle and Marshall et al. 2012). However, the underestimation of wind intensity is a known issue of reanalyses in other Antarctic regions (Tetzner and Thomas et al. 2019). ERA-interim covers the period 1979 to date and it has now been superseded by ERA5, the 5th generation product, which is higher resolution in time and space. Originally ERA-Interim ran from 1989, however a 10-year extension was later produced for 1979-1988 in 2011 (Dee et al. 2011). The model uses ERA interim u and v wind components at 3 hour intervals for the period 1989 to 2008, as well as other meteorological variables to compute the heat and freshwater fluxes at the surface.

2.2 Model Analysis

2.2.1 Key metrics

The wind field is connected to the stress acting on the surface and driving the distribution of Ekman flow (and hence regions of upwelling, location of oceanic fronts, etc.) and large-scale oceanic gyres. MLD is of importance as it reflects the water column stratification and affects the biogeochemistry in the surface ocean. MLD is a diagnostic measure of the surface ocean, representing the depth within which temperature and salinity, and hence density, are mixed. There are a few criteria to define MLD. “A commonly used criteria determines the depth where ‘critical temperature’ or density gradient corresponding to the top of the maximum property gradient is exceeded.” (Steele et al. 2009). In this study, MLD was calculated using density threshold of 0.01 kg m^3 (de Boyer Montégut et al. 2004; Anon et al. 2018). The effect of the wind on the surface ocean can be investigated with temperature and MLD.

2.2.2 Front identification and tracking

Frontal locations are tied both to the varying sea surface height field and the bottom topography, some to the temperature-based definition of the fronts (Russell et al. 2018), however several papers have used different ways to identify fronts from satellite and modelled data using surface variables: SST, SSS, sea surface height (SSH). In this thesis, fronts are defined/identified using a simplified version of Orsi et al. (1995) as used by Russell et al. (2018) for frontal definition in an inter-model comparison. To identify these areas of sharp gradients separating water masses, Orsi used hydrographic measurements. Below are how the two main fronts in the SO are identified in this study:

- To get the STF, the criteria of the surface 35.0 psu isohaline used by Belkin and Gordon et al. (1996) to define the southern STF, was used. One can equivalently use a temperature range between 10 and 12 °C and salinity range of 34.6–35.0 psu at 100 m depth as defined by Orsi et al. (1995).
- The SAF was located by taking the most poleward position of temperature at 400 m which are higher than 4 °C (simplified from Orsi et al. 1995 by Russell et al. 2018).
- The PF is identified by the equatorward position where the minimum temperature in the top 200 m is more than 2 °C, suggested by Orsi et al. (1995).

Using the above methodology, the SAF and PF fronts were located for each month from 1999 to 2008 for both models. This was repeated with the 2013 World Ocean Atlas (WOA13) climatology for comparison to the model as done by Russell et al. (2018). After identification of the frontal position in the model, the fronts were smoothed with a rolling mean (window = 6). In regions of high eddy kinetic energy such as off South America and the Agulhas Retroflection Region, identification of the STF required editing by hand: misidentified features were removed and missing values interpolated. Thereafter, annual climatological mean position of the front was calculated for both model and WOA and used to calculate the north/south anomaly for the period of study. The anomalies were then correlated with the SAM index to investigate the influence of SAM frontal location.

2.2.3 Regional timeseries analysis

Here, the seasonal cycles are presented in the form of a timeseries analysis for normalized metrics (Section 2.2.1) and the SAM index for regions described in Section 3.1.3. The data (oceanic variables) are deseasonalized by removing the monthly climatological mean and normalised using the formula:

$$z = (x - min(x)) / (max(x) - min(x))$$

Positive values of the SAM index correspond with stronger-than-average westerlies over the mid-high latitudes (50 °S - 70 °S) and weaker westerlies in the mid-latitudes (30 °S - 50 °S) (Marshall et al. 2005). The SAZ is the largest in high nutrient, low chlorophyll province in the world's oceans, also it is central to linkages between the ocean atmosphere CO_2 exchange and climate. The SAZ also represents a transition boundary between the warm, saline and the cold silicate rich waters South of the PF (Hernández et al. 2019), hence it is important to investigate how the SAM may influence these differences at these areas. We chose two boxes to represent these two latitude ranges, located within the SAZ and AZ (Figure 6). Longitude of the box was chosen to coincide with a known observation region in the SAZ (Swart et al. 2012).

Table 1: Location of boxes for timeseries analysis

	Longitude	Latitude
SAZ	7.5 to 9.5 °E	-44. to -42. °N
AZ	7.5 to 9.5 °E	-55. to -53. °N

2.2.4 Observational dataset

Model output are compared with in situ observational data from the WOA13 for frontal movement (Section 3.1.2) and seasonal cycle of a climatological year (Section 3.1.3). For comparison of climatological MLD (Section 3.1.3), we attempted to use data from argo profiles described in Holte et al. (2017), however the data was too spacious, particularly with respect to the size of the chosen 2 by 2 ° boxes, hence the gridded de Boyer Montegut et al. (2004) MLD dataset was used. However, the data is gridded at 2 °, thus for regional timeseries analysis only one profile was found at the local boxes described in Section 2.2.3 and so the mean MLD as used from this dataset may be biased against the model output.

2.2.5 Correlation with SAM index

One of the aims of this study is to investigate the influence of the SAM on modelled circulation and distribution of SST and SSS in the SAZ and AZ as a function of the numerical model spatial resolution. To study the response/relationship of the metrics (SST, SSS, MLD and frontal location) to the SAM, monthly averaged metrics are correlated with Marshall's station-based SAM index from 1998 to 2008 using Pearson's correlation coefficient (significant at $p < 0.05$) on all variables (Section 3.2.1) similar to previous SAM studies (Lovenduski and Gruber et al. 2005; Lefebvre et al. 2004; Hall and Visbeck et al. 2002).

3. Results

3.1 Model Climatology

3.1.1 SATLANTIC05 vs SATLANTIC12 Annual mean

Before investigating the relationships between large-scale patterns of SO climate variability and the mentioned oceanic variables in Section 2.2.1, it is worth reviewing some key climatological features found in the SO and how these features differ in the two model runs.

A comparison of annual-mean eddy kinetic energy (EKE), energy derived from the turbulent time-varying component of the ocean currents, for SATLANTIC05, SATLANTIC12, and satellite-derived EKE is shown in Figure 7. EKE is used as a measure of transient ocean features such as ocean eddies and meanders in the SO, contributing to the circulation of oceanographic variables thus affecting and/or driving their distribution. EKE is calculated by removing the annual climatological mean. As expected, SATLANTIC12 (Figure 7b) clearly shows mesoscale processes, e.g. the retroflection region of the Agulhas current and the region East of South America which shows high energy suggesting high (low and large-scale) eddy activity around the area whereas the SATLANTIC05 model is missing a lot of mesoscale processes and EKE in major eddying regions is not well represented. SATLANTIC12 at 8 km compares to satellite in resolving mesoscale eddies.

a) EKE model ½°

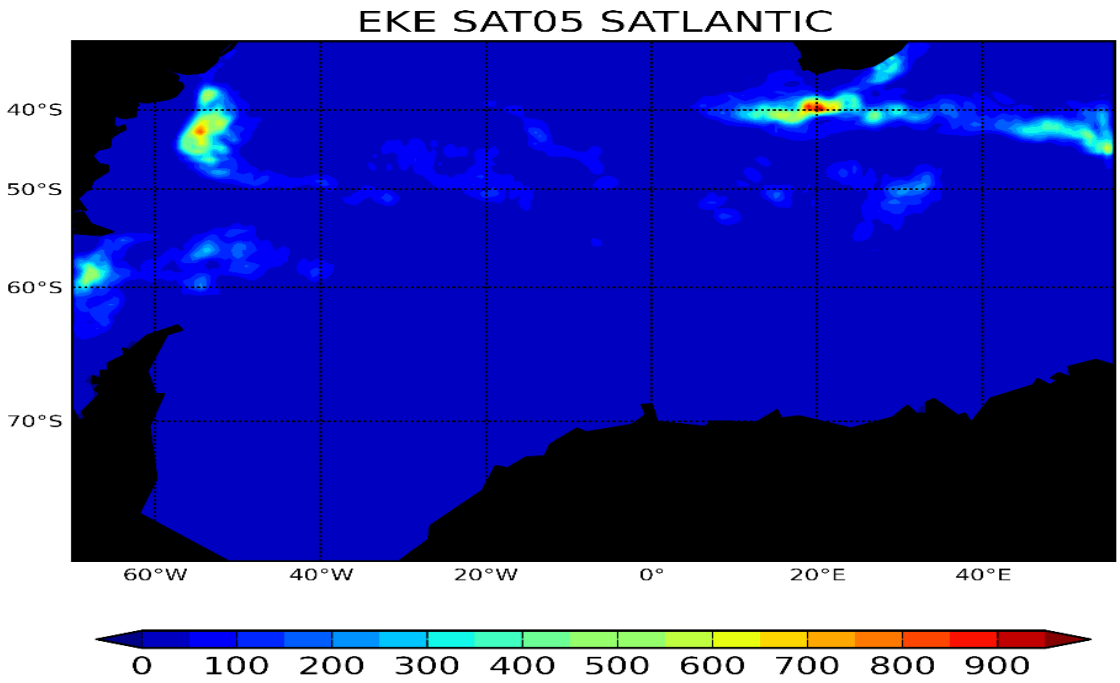

b) EKE model 1/12°

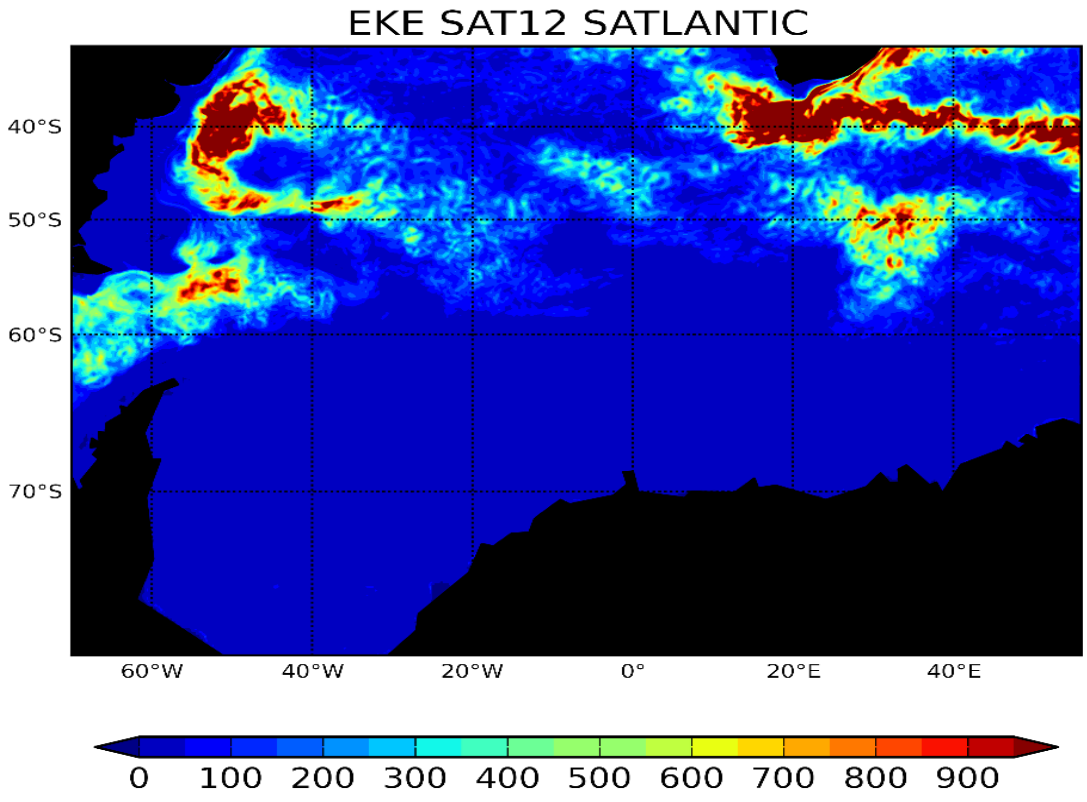

c) EKE Satellite

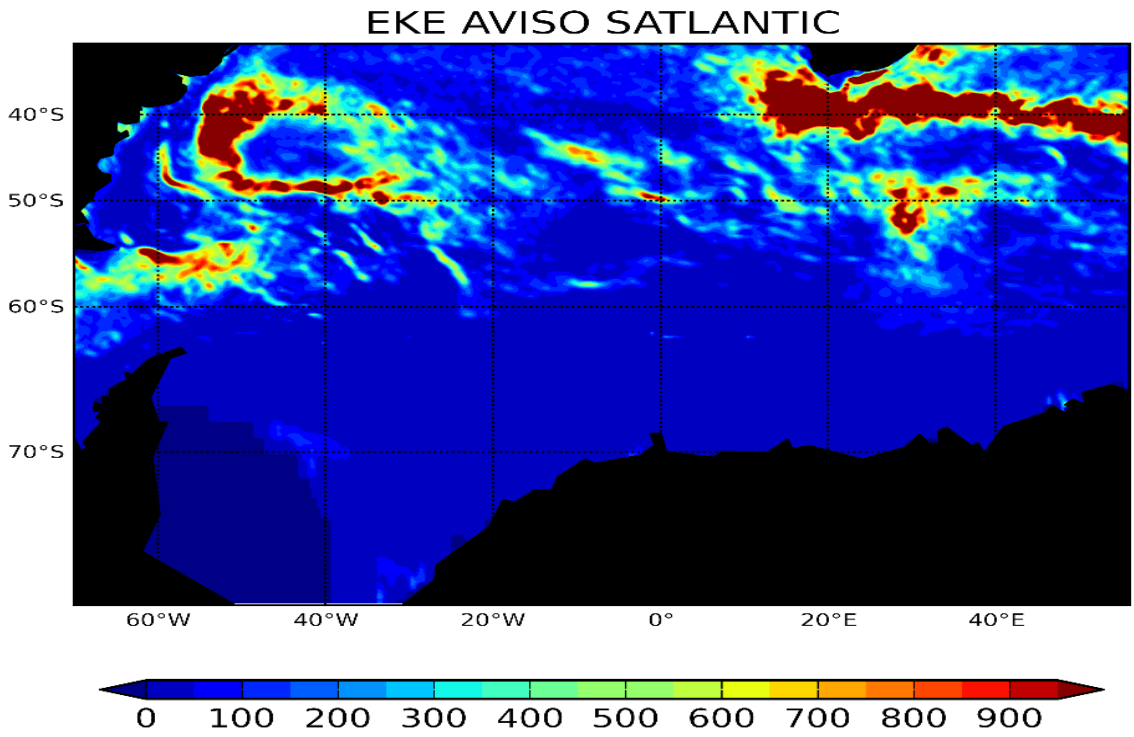

Figure 7: Annual mean eddy kinetic energy (EKE) for (a) SATLANTIC05 and (b) SATLANTIC12 compared to (c) AVISO satellite data.

SST in the SO typically decreases from north to south in three steps, with the SAZ (STF to the SAF) and Polar Front Zone (PFZ, SAF to the PF) ranging between 15 - 25 °C and 7 - 15 °C, respectively, and temperatures from the PF to the Antarctica being cooler between 0 - 5 °C (Demarcq et al. 2003). This temperature pattern is reflected in both models, with minor observable differences, related to model resolution, described in Section 4. Figure 8 shows annual mean SST from the climatology from 1999 to 2018 for both models: SATLANTIC05 (Figure 8a) and SATLANTIC12 (Figure 8b). In SATLANTIC12, SST patterns show clearer transitions between water masses of different temperatures than SATLANTIC05.

SSS gradient is known to be weak in the SO because of the lower temperatures and lesser evaporation. Seasonal differences of approximately 1 psu occur between the STF and SAF (Bulusu et al. 2017). Figure 9 depicts model outputs of annual mean SSS climatology. Both models show similar spatial patterns of SSS. North of the STF, SSS ranges between 34.5 - 36 psu, and from SAF to Antarctica varying between 33 and 35 psu. Some areas around the coast of Antarctica and South America show much lower SSS, which may result from ice melting and river discharge. In the eddy resolving model, there is a belt of mean SSS higher than surrounding areas, across the PF, which is not shown in the eddy permitting model.
Annual mean climatological MLD for the models is shown in Figure 10. The deepest mixed

layers are around the coast of Antarctica and the Weddell Sea (> 140 m) (between 30 and 60 °W), and just north of the ACC where Antarctic Intermediate Water (AAIW) and SAMW form. This is seen in both models, however, as mentioned before, some clear differences are seen between the models. In particular, the effects of small (and large) scale eddy activity in contrast to the eddy-permitting: i.e. deep MLD hotspots around ACC appear clearer with increased resolution. This plays an important role in the dynamics and thermodynamics of the SO (Morrow et al. 2010). Also, deep mixed layers follow the PF. This is also true for the SAF, clearly seen in the eddy resolving model.

a)

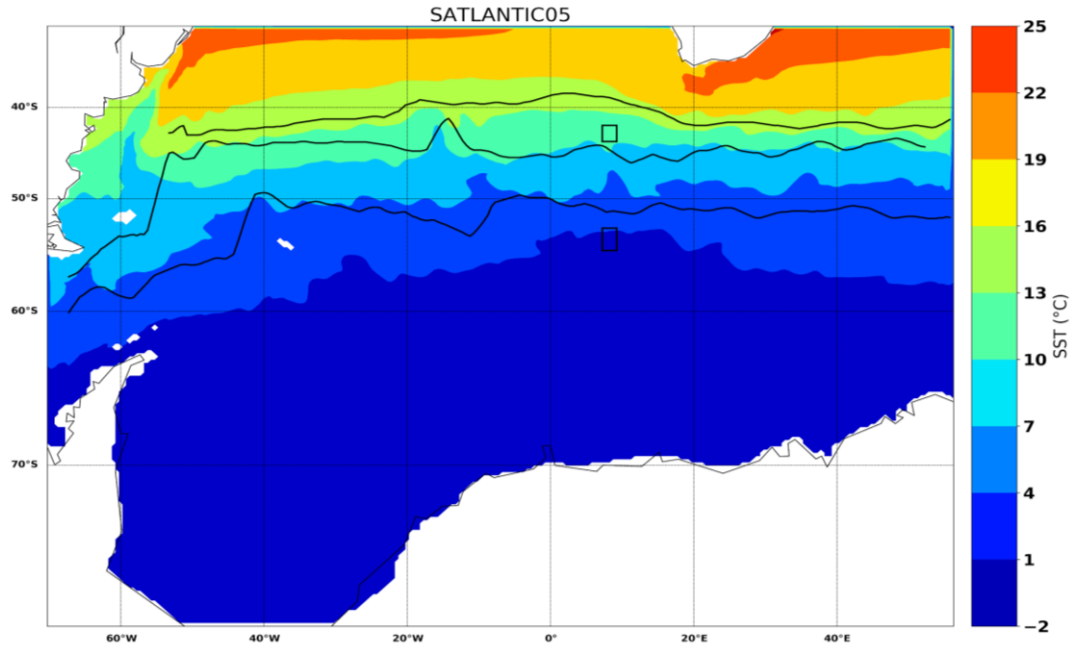

b)

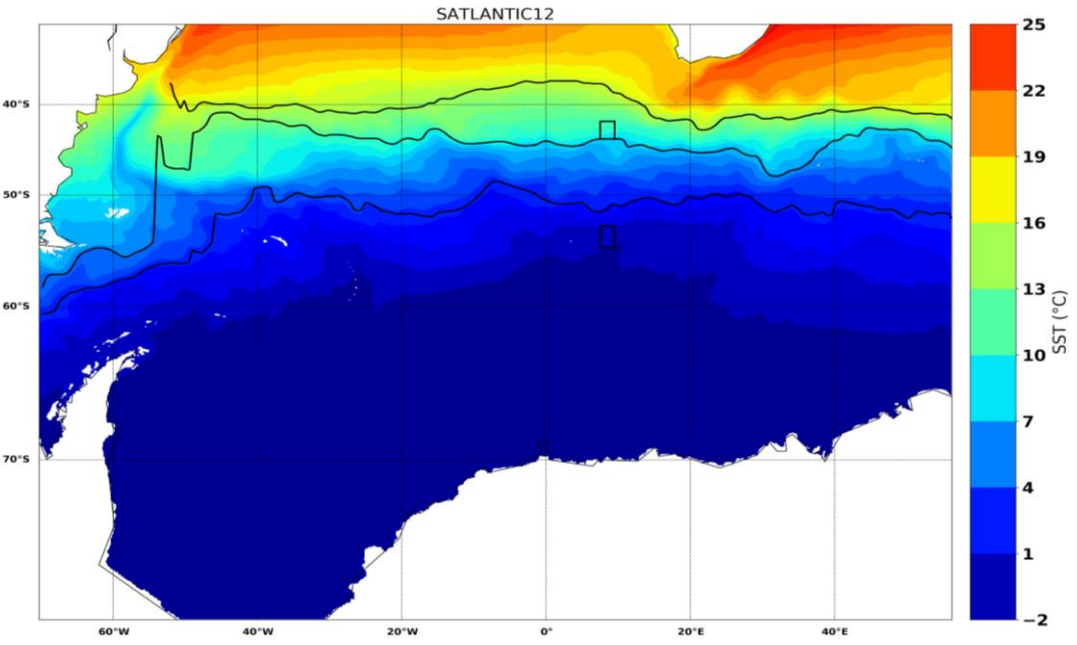

Figure 8: Annual mean climatological SST for models: (a) SATLANTIC05 and (b) SATLANTIC12, with annual-mean climatological fronts overlaid as black lines.

a)

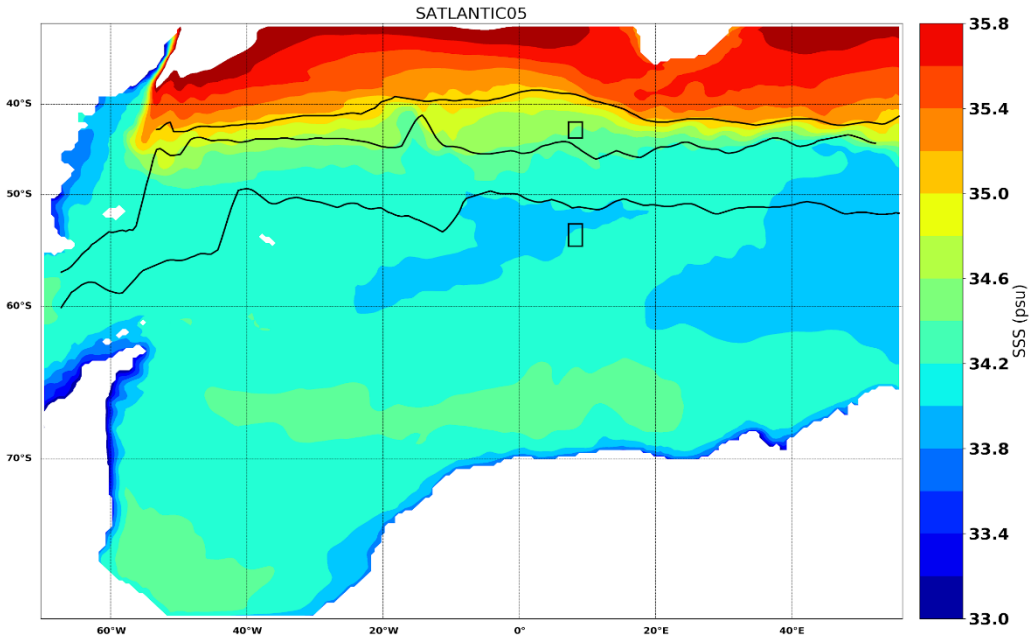

b)

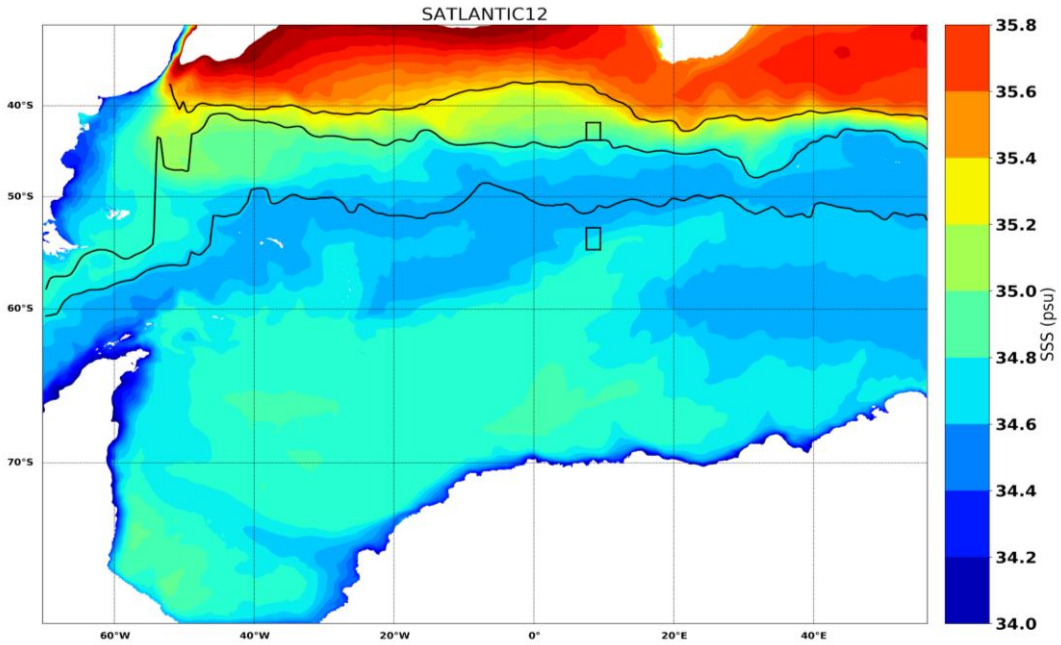

Figure 9: Annual mean climatological SSS for models (a) SATLANTIC05 and (b) SATLANTIC12, with annual-mean climatological fronts overlaid as black lines

a)

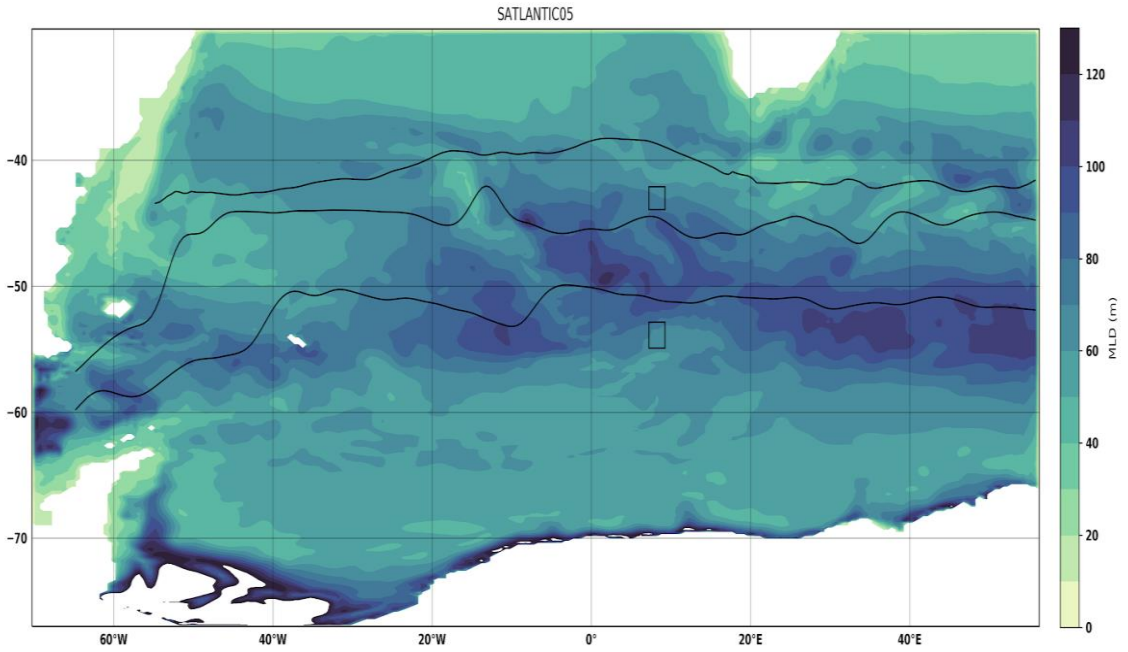

b)

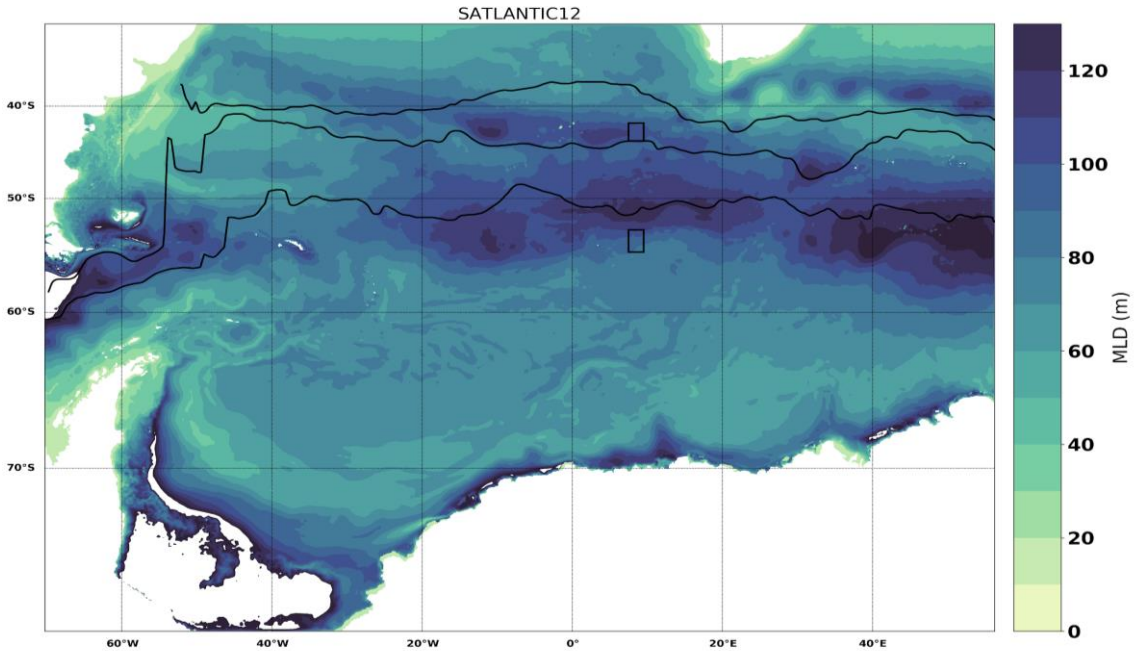

Figure 10: Annual means of the mixed-layer depth (MLD) for models (a) SATLANTIC05 and (b) SATLANTIC12, with annual-mean climatological fronts overlaid as black lines.

3.1.2. Subantarctic and Polar Front location

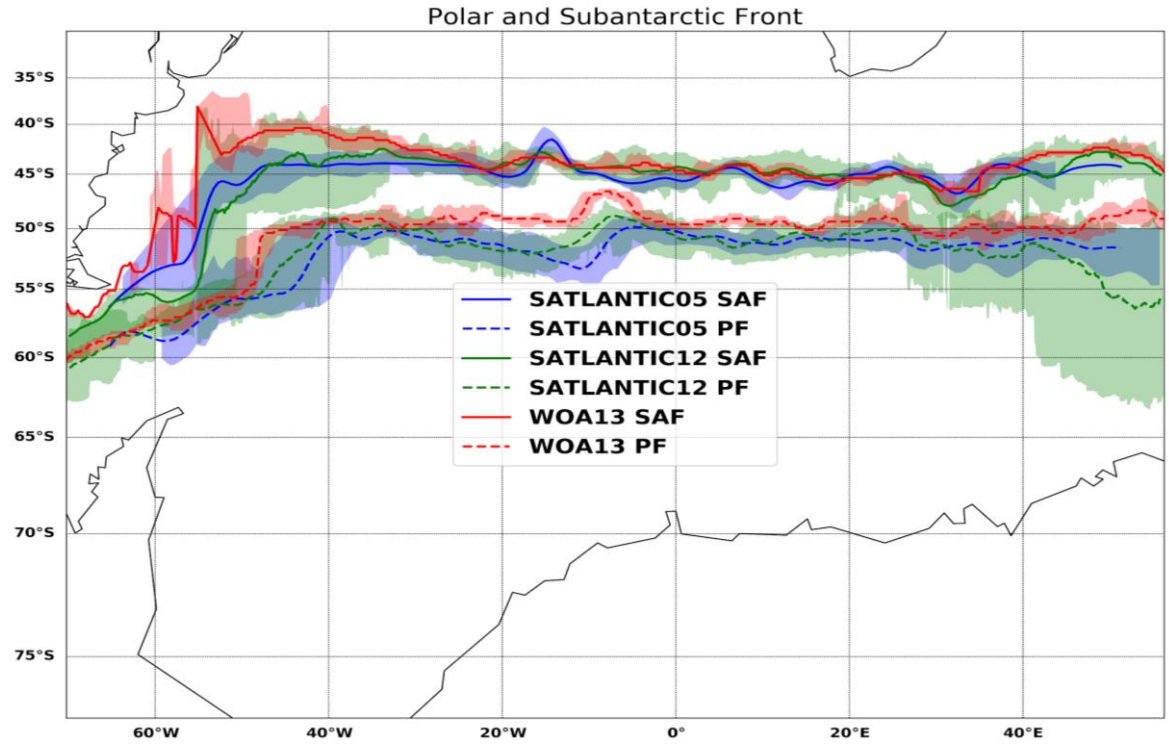

Figure 11: Annual-mean climatological fronts (solid and dashed lines) with north-south location of the minimum and maximum monthly-mean frontal latitude overlaid (shaded region) for SATLANTIC05, SATLANTIC12 and WOA13.

Figure 11 shows the monthly mean location range of the Polar Front (dashed) and the SAF (solid) as determined from the observations (WOA13) and model simulations (SATLANTIC05 and SATLANTIC12). Monthly movements of the model-mean frontal positions are not far off from fronts calculated from the WOA13 data except for some regions, for example: regions of high eddy kinetic energy (area at 40 - 60 °W and from 20 °E). Mean annual fronts of the eddy permitting and resolving models follow a similar pattern as the WOA13 data, however the distance between the annual fronts are greatest when comparing model versus WOA13 especially the PF, where WOA13 shows a more northward PF, followed by the SATLANTIC12 and then SATLANTIC05 to the south. SAF has similar frontal patterns between models and WOA13, except also at high eddy kinetic energy areas, such as east of South America. Mean monthly frontal movement is greatest in the eddy-resolving model. Also, oceanic fronts show latitudinal differences in their annual mean location of up to 3 ° between the models in the domain, i.e. areas around 40 - 60 °W and 15 - 20 °W.

3.1.3 Seasonal cycle of a climatological year

In this section the impact of model resolution on the seasonal cycle is evaluated for two different sites in the SAZ and in the AZ as marked by black boxes on the figures above (also see Figure 6 and Table 1). As explained in the Introduction (Section 2.2.3), the winds show different patterns during a positive SAM in these regions. Thus, at these two latitudes, the influence of the SAM should be readily noticeable in the modelled ocean variables.

Seasonal cycles of SST in the SO typically range between -2 and 11 °C, reaching a yearly peak in Southern Hemisphere summer (Wolf et al. 2013). Figure 12 shows the model seasonal cycle of SST for the two resolutions. In the SAZ average SST are between 7 and 10 °C, while in the AZ mean SST ranges between -2 and 1 °C, with very minor difference between the two model resolutions. Generally, both models are cooler than WOA13. Although in the SAZ (Figure 12a), the eddy-resolving model output is more consistent with WOA13. Both models show a clear seasonal cycle, however, at the SAZ, SATLANTIC12 shows a lag of about a month to reach the lowest temperatures and thereafter warm. This is not the same for the AZ: maximum and minimum temperatures occur at approximately the same time, although SATLANTIC minimum SST is lower than in SATLANTIC05. This is not the same for SSS.

Figure 13 depicts climatological SSS for the SAZ and AZ for the period of study. Although the models show similar spatial and timeseries patterns, the SSS signal show differences between the models. In the SAZ, SSS values vary from 34.3 to 34.5 psu throughout the year, seen in both the coarse and eddy-resolving model. In the SAZ (Figure 13a), SATLANTIC12 shows a more variable SSS signal, the climatological signal for this model only range between 34.33 (in May) and 34.36 psu in February and again in August, whereas SATLANTIC05 shows a smoother seasonal cycle, ranging between 34.36 (April) and 34.5 psu in October/November. In the AZ (Figure 13b), the mean climatological SSS in summer ranges between 33.9 and 34.2 psu and gradually increases to a peak of over 34.1 psu in September. Mean SSS from SATLANTIC models are also in agreement with WOA13 data, however in WOA13 mean SSS signal is more variable. For instance, in the SAZ (Figure 13a) the mean SSS signal from WOA13 shows a rapid increase in April which is not reflected in the SATLANTIC models. Mean SSS signals at the AZ show a clear seasonal cycle. Changes are first captured by the coarse model, SATLANTIC05: in September, SSS decreases before SSS of SATLANTIC12; this lag is not seen for the SAZ SSS seasonal cycle.

Seasonal cycles of the MLD in the SAZ and AZ have a similar seasonal pattern for both models, as seen in Figure 14. The MLD range of the two models are also similar to that of de

Boyer Montegut MLD dataset. The lower resolution model however, exhibits shallower MLD signals than the high resolution model. The greatest differences of MLD signals between models is readily seen in AZ (Figure 14b). On average, MLD ranges from 40 m to a maximum of 110 m throughout July and August for SATLANTIC05 and SATLANTIC12 respectively, in the AZ (Figure 14b). In the SAZ however (Figure 14a), the MLD is shallower from October to April ranging between 20 and 80 m, and peaks in July/August at depths of 175 m are in line with seasonal warming patterns. Also, changes in MLD signals in the SAZ show a temporal lag between the models, SATLANTIC05 reaches maximum depth a month earlier than SATLANTC12, while SATLANTIC12 is consistent with observations.

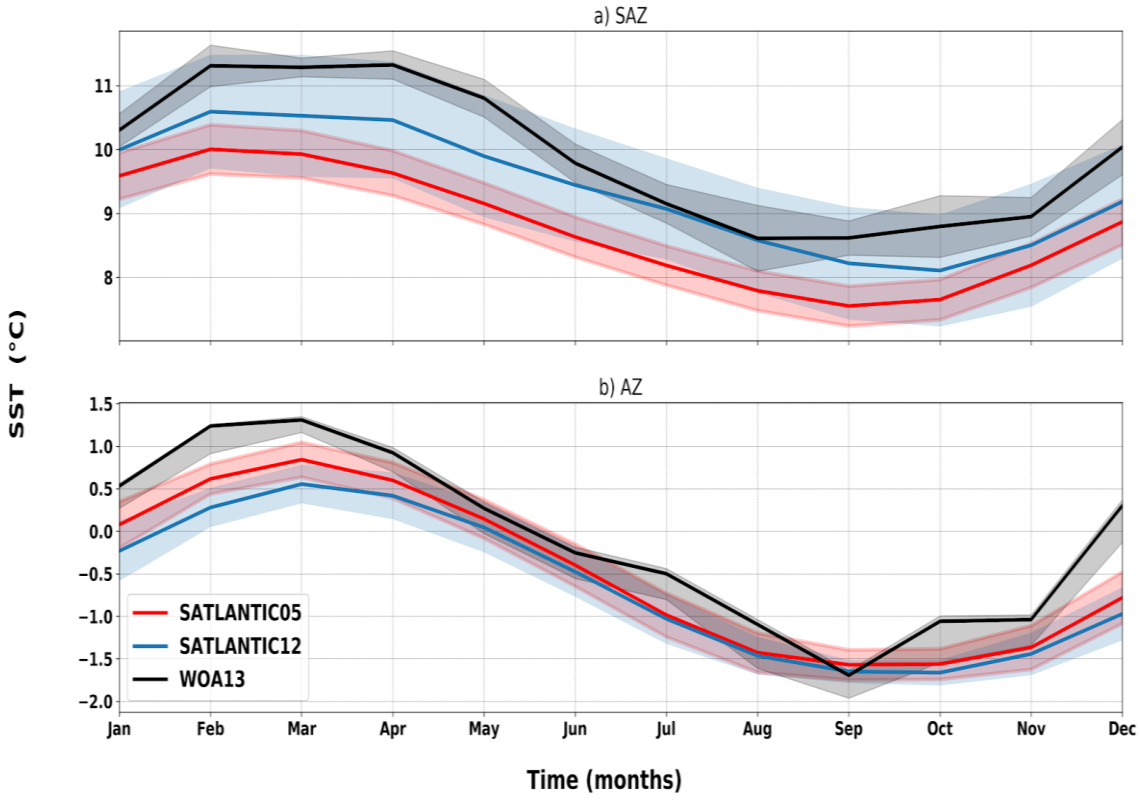

Figure 12: Monthly mean climatological seasonal cycle of SST and standard deviation (shading) for models SATLANTIC05 and SATLANTIC12 (shown in green and blue lines, respectively) for a) SAZ and b) AZ.

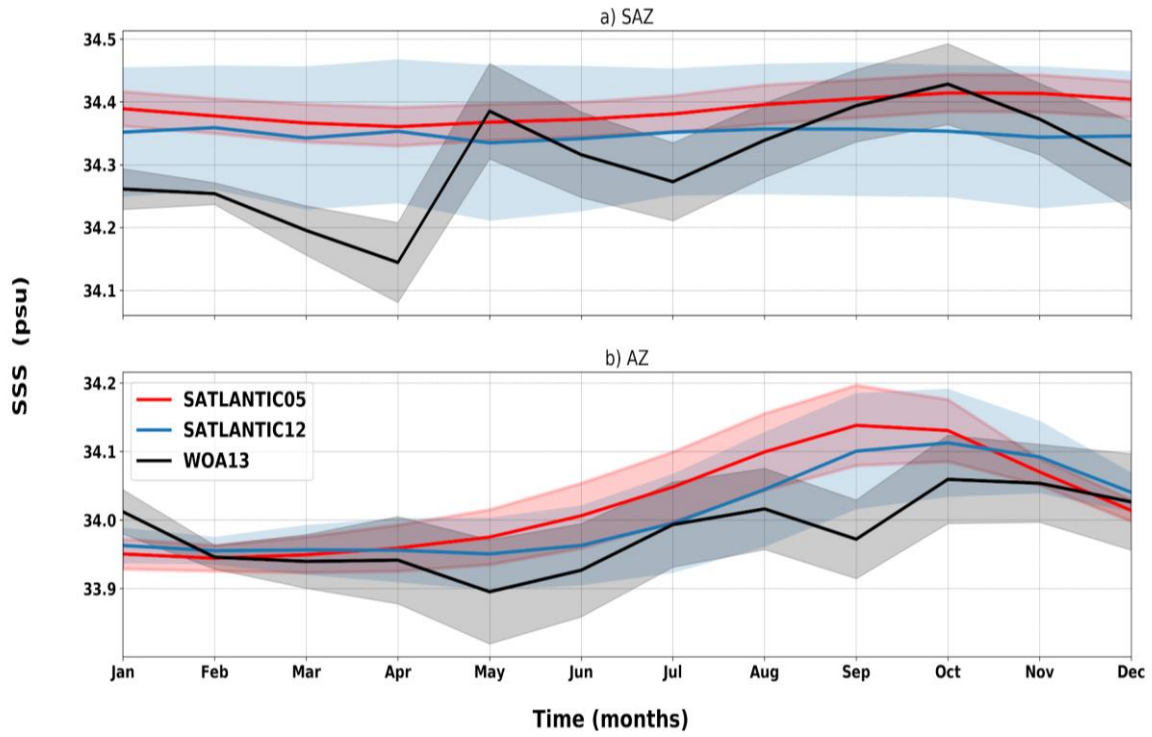

Figure 13: Monthly mean seasonal cycle of SSS and standard deviation (shading) for models SATLANTIC05 and SATLANTIC12 (shown in green and blue lines, respectively) for a) SAZ and b) AZ.

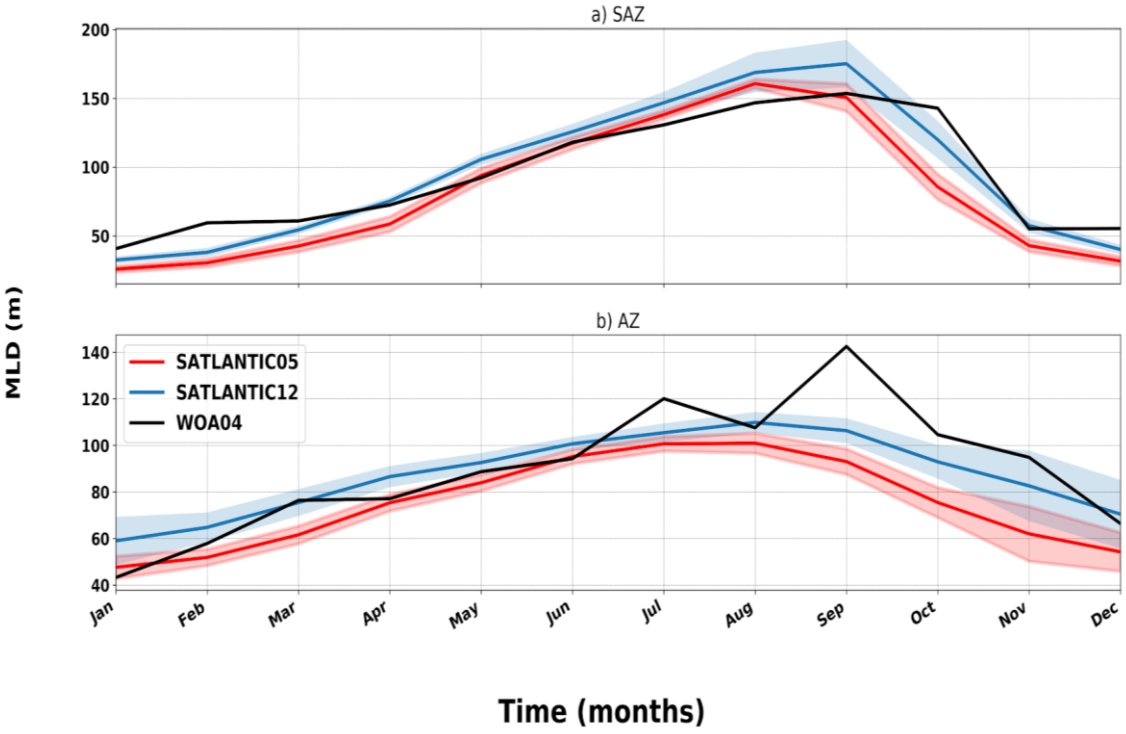

Figure 14: Monthly climatology for mixed-layer depth (MLD) and standard deviation (shading) for models SATLANTIC05 and SATLANTIC12 (shown in green and blue lines, respectively) for a) SAZ and b) AZ.

3.2 Role of the SAM in the Southern Ocean

3.2.1 Correlation: SAM index and model variables

To verify the influence of the SAM index on the surface ocean and the mixed layer, the SAM index is correlated with oceanographic variables: wind speed, SST, SSS, and MLD as shown below in figure 15, 16, 17 and 18. Regions where the correlation is more positive means if the SAM increases, then the oceanic variable in that area would follow closely in an increasing pattern, or vice versa, i.e. an increase/decrease in the SAM index tends to intensify/weaken westerlies and a decrease in the SAM index would weaken westerlies in the SO. Regions where the correlation is negative means that the SAM index and wind speed are inversely proportional - i.e. an increase in SAM signal coincides with a decrease in said variable, or vice versa. Figure 16 shows that the correlation between the SAM index and wind speed is negative (up to 0.8 ($p < 0.05$)) poleward from 50 °S, with negative correlations around the SAF and STF (up to - 0.6) and around the coast of Antarctica. Moreover, correlation patterns are relative to mean frontal position, so that correlations between SAM and oceanographic variables differ in regions between fronts (frontal zones). The zero correlation region is found around 50 °S, and another one is visible at 70 °S. These results are consistent with findings by Lovenduski and Gruber. (2005, their Figure 4), who used satellite products and are discussed in the next chapter.

The connection between SST and the SAM index can be observed in patterns of correlations between the SAM index and SST climatology. Figure 16 shows the correlation between monthly SAM index and monthly SST data from models (a) SATLANTIC05 and (b) SATLANTIC12. The models show similar correlation patterns to each other i.e. the correlation between SAM index and SST in the domain is positive northward of 55 °S, with strong negative correlations around the Weddell Sea, consistent with previous studies (Kostov et al. 2017, and references therein). Small differences are evident between the models. Furthermore, there is a negative correlation in the area between PF and AZ on both models, however these correlation patterns are intensified on the eddy permitting model, evident in the area at 40-60 °W, 20 °E and at the Weddell Sea. The former coinciding with EKE patterns highlighted in section 3.1.1.

Figure 17 shows correlation patterns of SSS and the SAM index for the models being analysed. The models show similar maps of positive correlations (up to 0.8, $p<0.05$) north of 60 °S, as seen in Figure 16. A band of positive correlation, just south of PF is evident in the model, which separates the areas of positive and negative correlations. The area south of this belt of positive correlation is followed by a negative correlation of up to - 0.3, and - 0.5 for SATLANTIC05 and SATLANTIC12, respectively, down to Antarctica.

Presented in Figure 18, are correlation maps of the SAM index and MLD for models (a) SATLANTIC05 and (b) SATLANTIC12, showing an overall negative correlation of over ± 0.4 and ± 0.8, respectively in the domain. A band of strong negative correlations occur between the PF and the STF and some areas on the coasts, while a belt of positive correlation of up to + 0.4 on Figure 18a and + 0.8 in b) is evident south of the PF (at the northern extent of the AZ), latitudes where the westerlies respond to the positive SAM.

Generally, the spatial distribution of correlations between the SAM and SSS, winds speed and MLD is similar for both models (Figure 15, 16, 17, and 18). However, a stronger SAM correlation is seen in regions where westerlies respond to the positive phase of the SAM. Furthermore, the eddy resolving model shows SAM correlations resolved more regionally (higher localised response) compared to the eddy permitting model (SATLANTIC05).

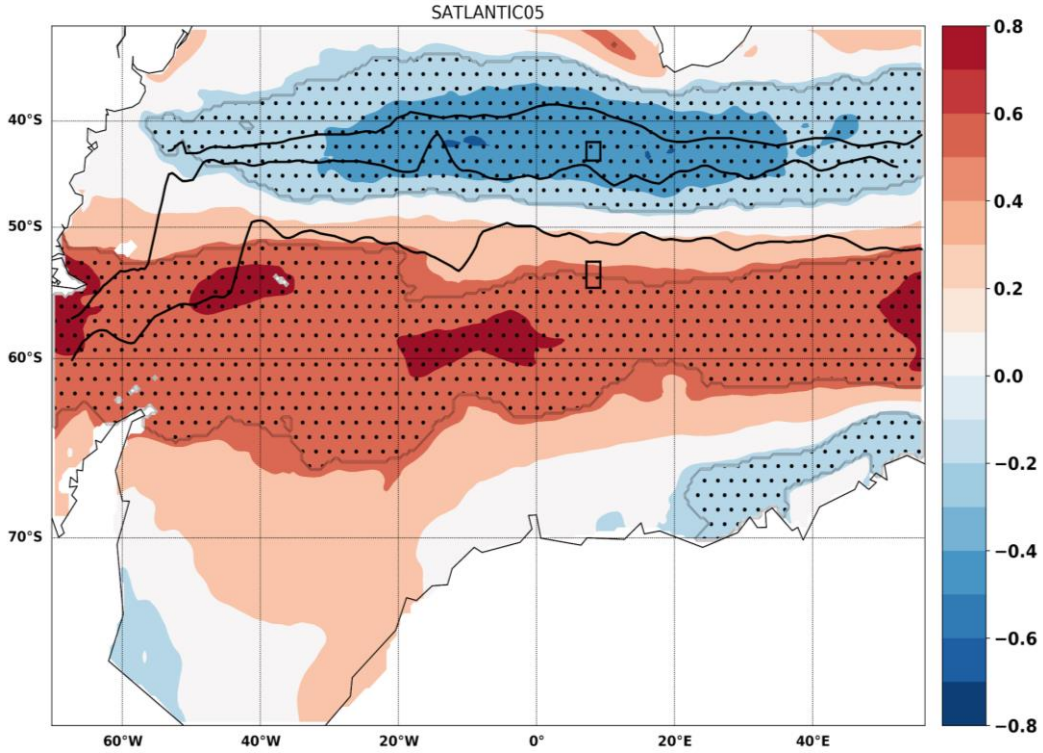

Figure 15: Correlation maps of wind speed and the SAM index for SATLANTIC05. Bold black lines represent the position of the mean fronts from north to south: STF, SAF and PF. Black contour lines and dots show the significance of the correlation at p<0.05.

a)

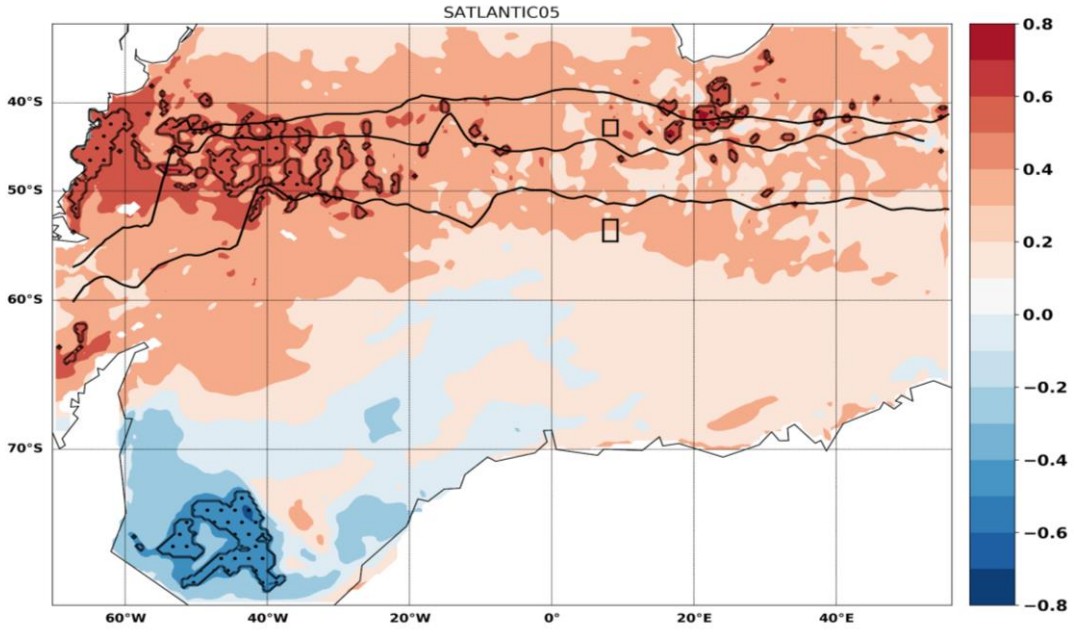

b)

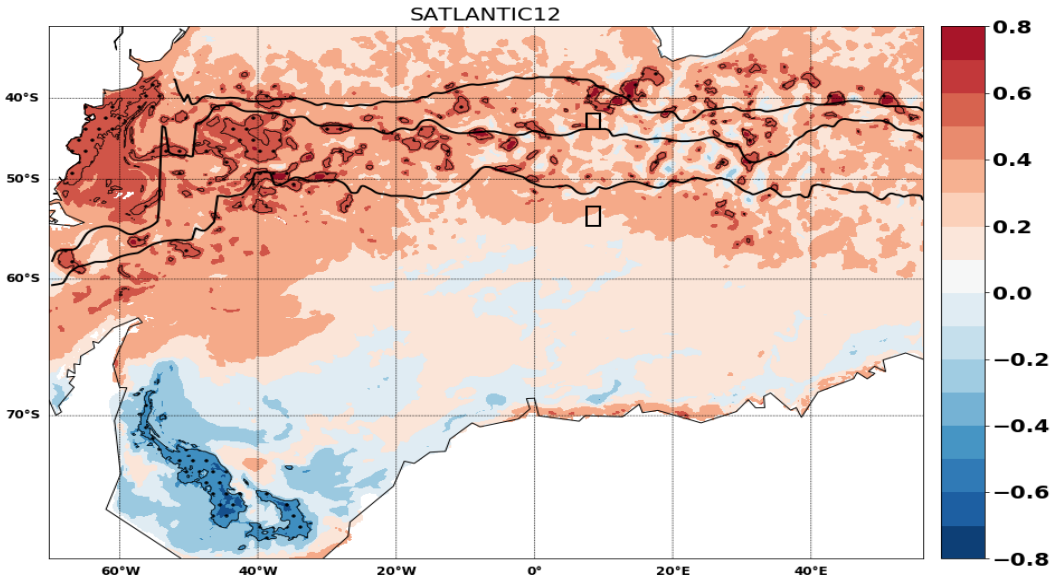

Figure 16: Correlation maps of SST and the SAM index for models (a) SATLANTIC05 and (b) SATLANTIC12. Bold black lines represent the position of the mean fronts from north to south: STF, SAF and PF. Black contour lines and dots show the significance of the correlation at $p < 0.05$.

a)

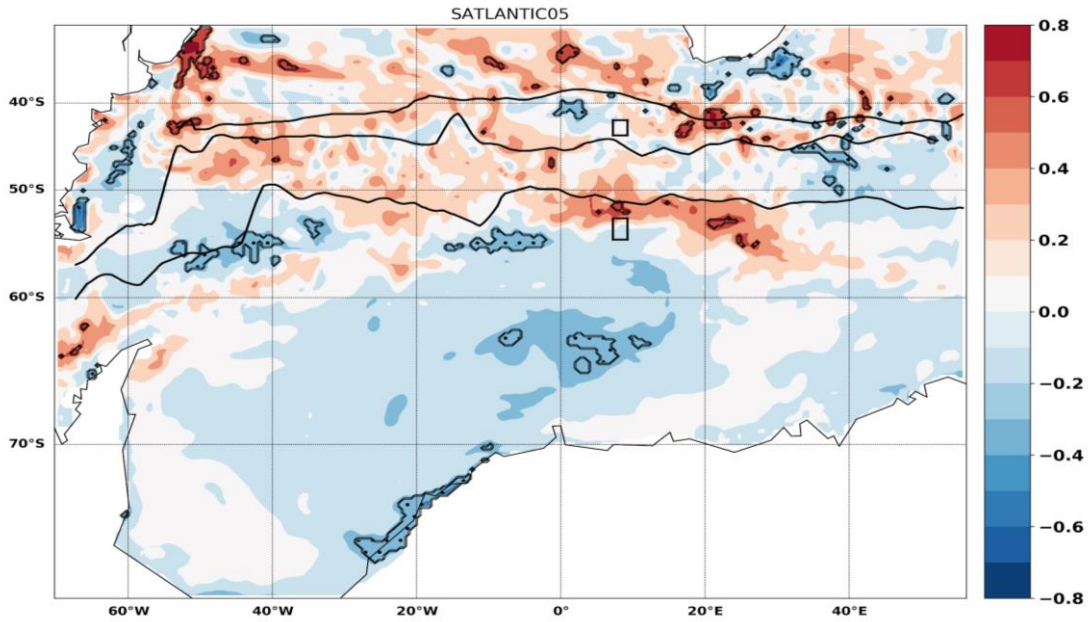

b)

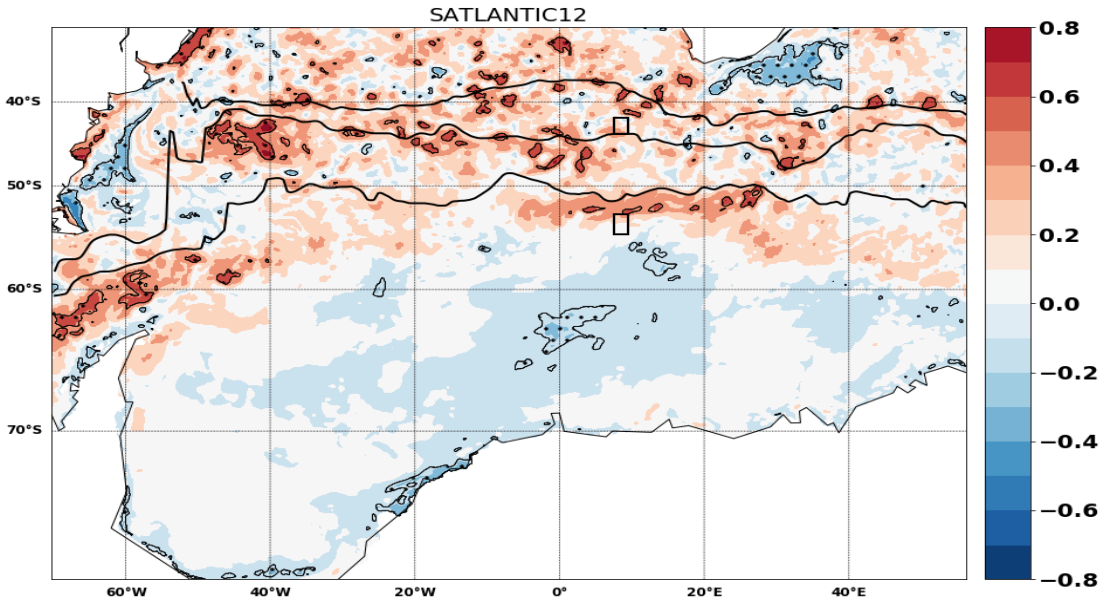

Figure 17: Correlation maps of SSS and the SAM index for models (a) SATLANTIC05 and (b) SATLANTIC12. Bold black lines represent the position of the mean fronts from north to south: STF, SAF and PF. Black contour lines and dots show the significance of the correlation at $p < 0.05$.

a)

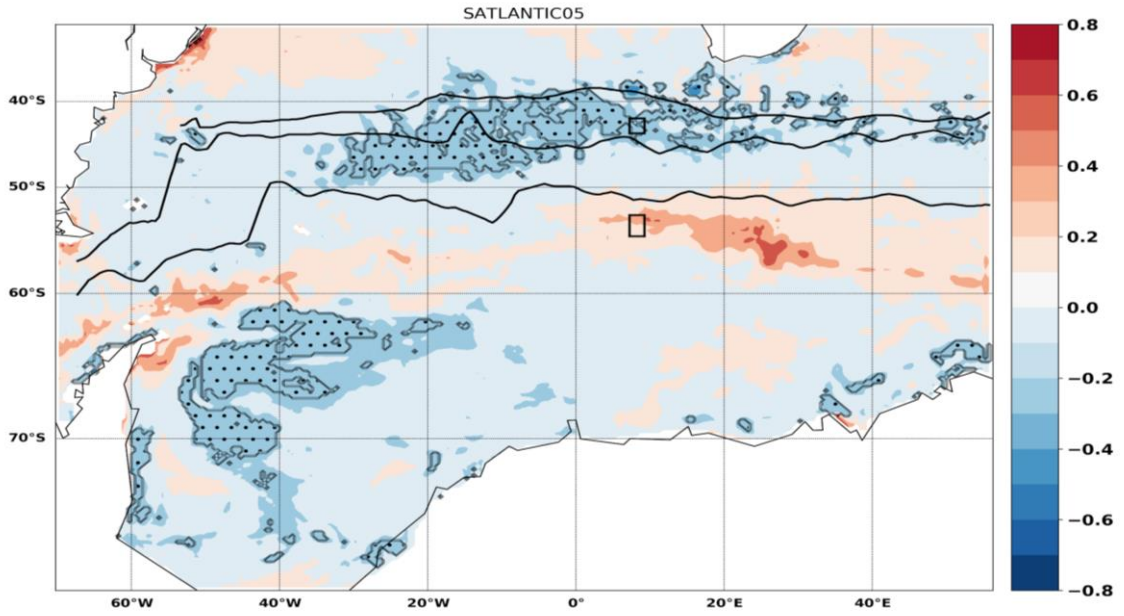

b)

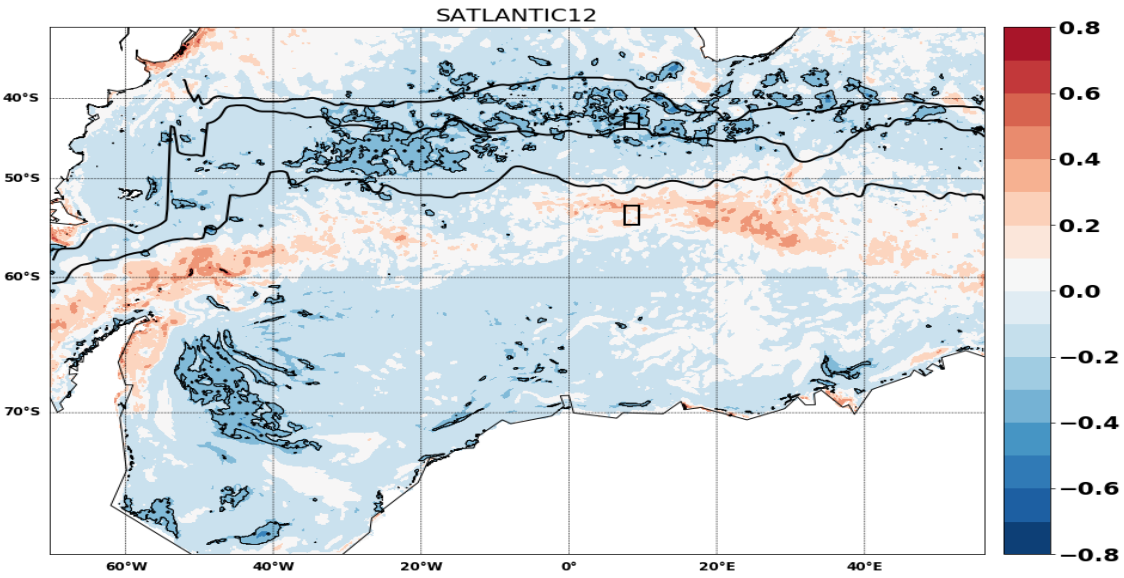

Figure 18: Correlation maps of mixed-layer depth (MLD) and the SAM index for models (a) SATLANTIC05 and (b) SATLANTIC12. Bold black lines represent the position of the mean fronts from north to south: STF, SAF and PF. Black contour lines and dots show the significance of the correlation at $p < 0.05$.

3.2.2 Correlation: SAM index and frontal position

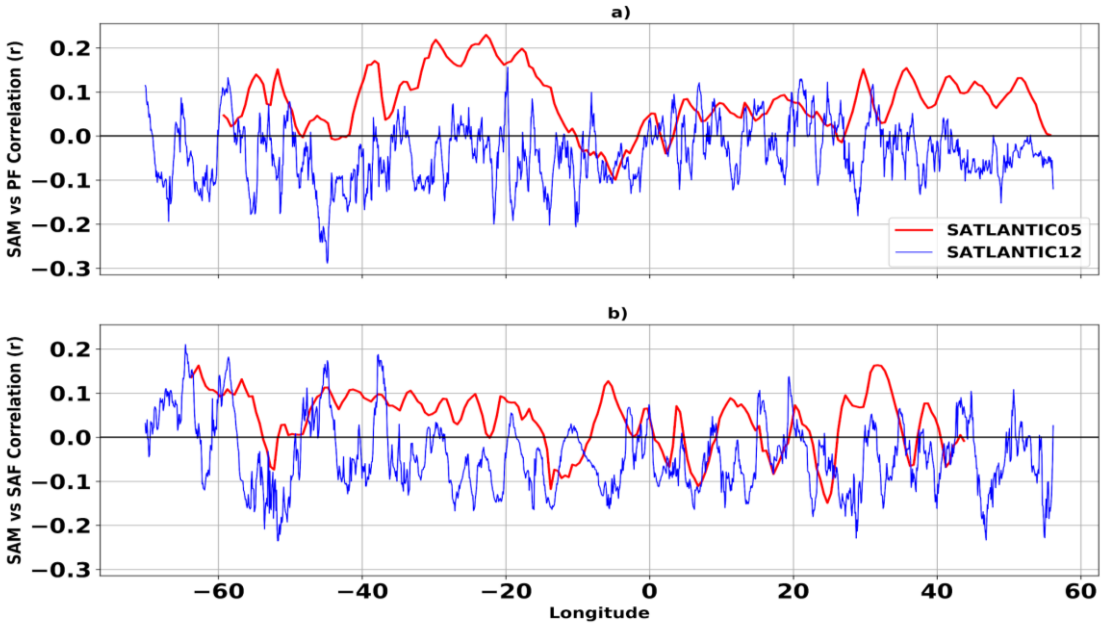

Figure 19: Model correlation coefficient of annual frontal north/south latitudinal anomaly vs SAM index ($p < 0.05$) for each grid point along domain longitude.

Figure 19 shows the correlation coefficient of the SAF and PF latitudinal anomaly versus the SAM index at each model longitude. The correlations are low ($r < \pm 0.3$), showing that the influence of SAM on mean monthly movement of fronts is minimal. The eddy-permitting model, SATLANTIC05, frontal position anomaly shows mostly positive correlation to SAM, i.e. northward latitude anomaly correlates with positive SAM, predominantly for the PF. In contrast, correlations for the eddy-resolving, SATLANTIC12 are for the most part negative and weaker and more spatially variable.

3.2.3 Time series analysis in the representative boxes

One of the aims of this thesis is to investigate how wind variability in the SO driven by large scale climatic patterns influence the upper ocean representation at coarser and finer spatial scales. This section presents time series for mean SST, SSS, MLD and wind speed at the selected boxes (Section 2.2.3). A timeseries analysis helps highlighting events which may have been influenced by the SAM.

Figure 20 shows mean monthly SST-SAM index timeseries for SATLANTIC05 and SATLANTIC12 in the SAZ and AZ region for the period of the study (1999-2008). Mean SST signals in the SAZ and AZ boxes are in and out of phase with the SAM index for both models, confirming low SST-SAM index correlations in Section 3.2.1. Furthermore, models exhibit some differences in SST signals, especially in the SAZ where SST signals from the eddy-permitting model lags behind that from the eddy-resolving model. The coarse model shows SST signal peaks that are higher than the eddy resolving model in some years (2000 and 2003 - 2007) in the SAZ.

Figure 21 shows Standardized mean SSS for the a) SAZ and b) AZ for SATLANTIC05 and SATLANTIC12. Mean SSS signals were in phase with the SAM until 2002, where mean SSS signal is highest in the SAZ for the eddy-resolving model, this peak is however seen in 2004 for the eddy-permitting model. In the AZ mean SSS signal is in and out of phase with the SAM index and lowest in 2002 for both models. Also SSS signals for the models have similar patterns, however in the SAZ, the low SSS could be related to a seemingly anomalous interaction between La-Niño and SAM in the Pacific Ocean in 1998-2000 (Morrow et al. 2010; Sallée et al. 2008). Hereafter, the SAM and SSS in the SAZ and AZ no longer oscillated in phase, after 2007, SAM and SSS signals were back in phase.

Figure 22 shows time series of mean standardized monthly MLD signals in the SAZ and AZ for SATLANTIC05 and SATLANTIC12. MLD in the SAZ and AZ are in and out of phase for this period, with the mixed layer in the AZ deeper than in the SAZ. The positive phase of SAM is associated with a deeper mixed layer at AZ and more shallow at the SAZ. The MLD signals do not show a lag between models like other variables, the models rather exhibit similar patterns at AZ. However, at the SAZ, MLD signals exhibit a few differences in the pattern of the signal between SATLANTIC05 and SATLANTIC12.

Figure 23 below shows that an out of phase relationship exists between the SAM index and wind speed at the two boxes, for the study period, confirming strong negative (~ -0.4) correlations table 2. Wind speed at SAZ and AZ have an in and out of phase relationship, were in phase in 1999-2002, 2004, 2007.

The correlation between the SAM and the upper ocean (SSS, SST and MLD) at SAZ and AZ range between +/- 0.2 for both models (Table 2) and thus not significant, except wind speed - SAM correlation ($r = -0.4$, $p < 0.05$) at SAZ. This result is in qualitative agreement with the one obtained by Hall and Visbeck (2002) and Lefebvre (2004), smaller in magnitude in this thesis.

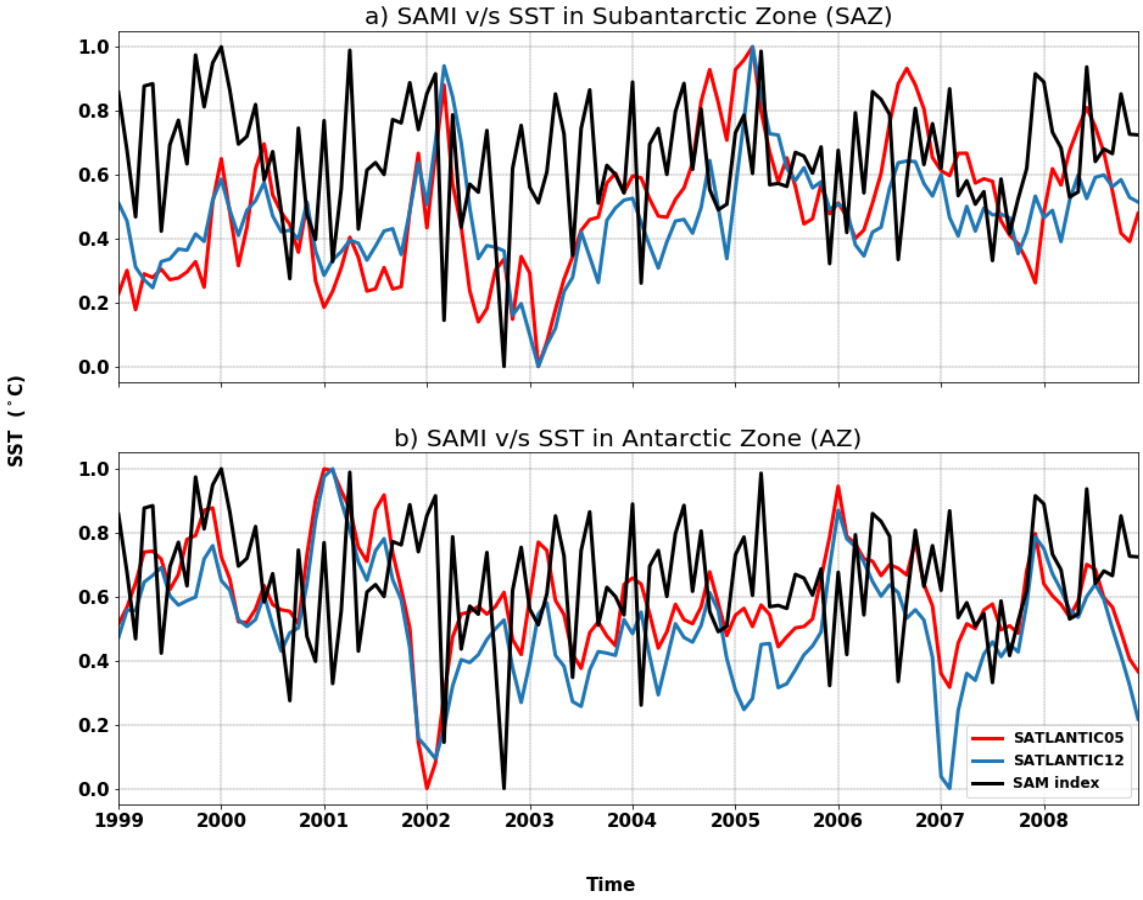

Figure 20: Timeseries (1999-2008) for standardized SAM index (black) vs standardized SST in a) SAZ and b) AZ for SATLANTIC05 (red) and SATLANTIC12 (blue).

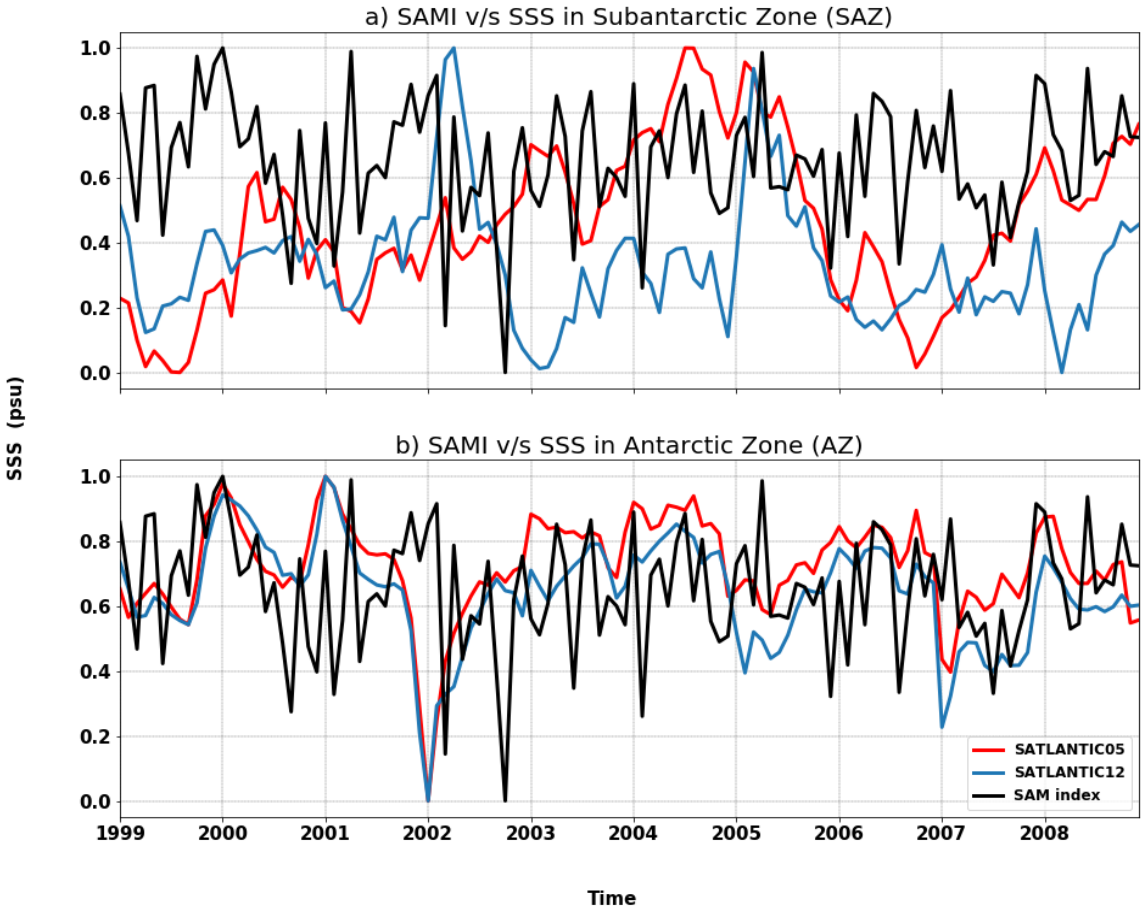

Figure 21: Timeseries (1999-2008) for standardized SAM index (black) vs standardized SSS in a) SAZ and b) AZ for SATLANTIC05 (red) and SATLANTIC12 (blue).

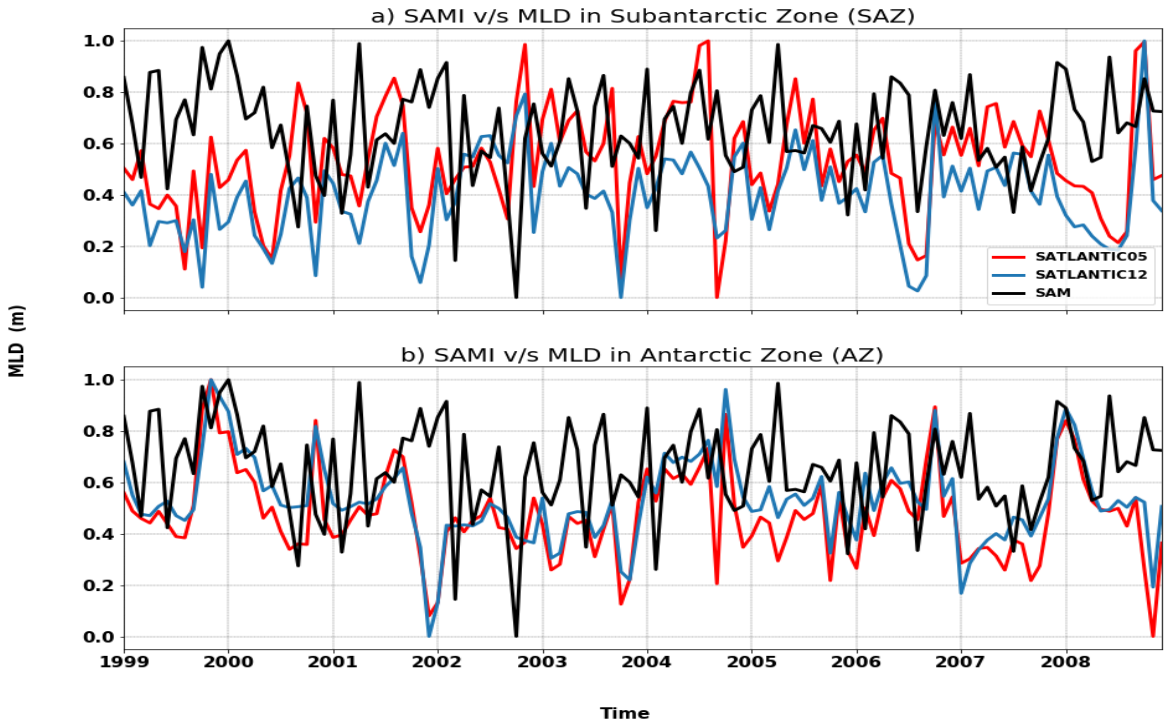

Figure 22: Timeseries (1999-2008) for standardized SAM index (black) vs standardized MLD in a) SAZ and b) AZ for SATLANTIC05 (red) and SATLANTIC12 (blue).

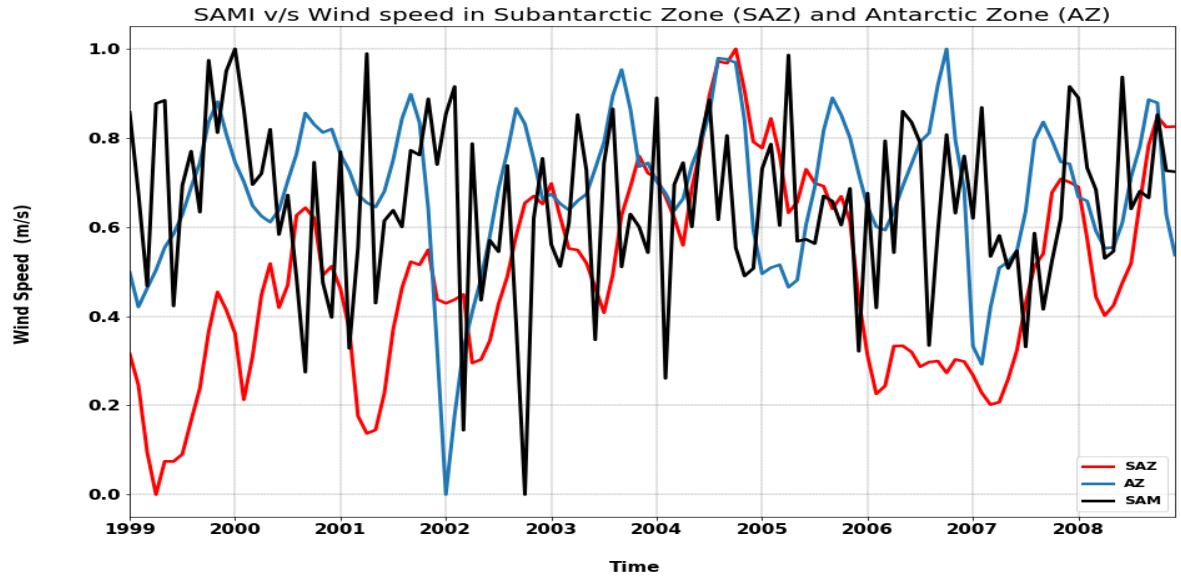

Figure 23: Timeseries (1999-2008) for standardized SAM index (black) vs standardized wind speed in SAZ (red) and AZ (blue) for SATLANTIC05.

Table 2: A correlation analysis between the SAM index and metrics at SAZ and AZ using models: SATLANTIC05 and SATLANTIC12.

Model	**SATLANTIC05**				**SATLANTIC12**			
Region	SAZ		AZ		SAZ		AZ	
Correlation	R	P value	R	P value	R	P value	R	P value
MLD	-0.159	0.082	0.223	0.0144	-0.167	0.0683	0.204	0.0255
SST	0.017	0.853	-0.0175	0.849	0.0492	0.593	-0.00798	0.931
Wind speed	-0.404	4.7e-06	0.182	0.0460	-0.167	0.0710	-0.153	0.095
SSS	-0.0183	0.843	0.0246	0.790	0.0324	0.725	0.0832	0.366

3.3 Summary

The above results confirm previous findings from studies done on the influence of the SAM on the SO, that a strong relationship exists and is replicated by the model. Although not significant, the SAM index has a higher correlation with wind speed at AZ than SAZ. This is expected during positive SAM. However, correlation analyses show that the strongest SAM influence is regional. Moreover, the correlation between the SAM index and surface variables: SST and SSS are more positive in areas where SAM is negatively correlated with wind speed (northward of SAZ) and regions of negative correlations between SAM and surface variables coincides with regions where wind speed is positively correlated with SAM (south of AZ), seen in both models (Section 3.2.1). These correlations between SAM and the selected variables at these selected locations confirms that the SAM index coincides with cool surface temperatures at higher latitudes and a weak cooling at mid-latitudes during positive phase, this differs regionally and is reflected in Sections 3.1.3 and 3.2.2 (Lovenduski and Gruber et al. 2005, Hall and Visbeck et al. 2002 and Lefebvre et al. 2004).

4. Discussion

The SO climate has been changing rapidly over the past several decades, on average the SO has warmed and freshened at about twice the average rate of the global ocean (Swart et al. 2018). However, the drivers of these changes are poorly understood, owing to sparse observational sampling. Some of these changes have been linked with modes of variability in the SO such as ENSO, SAM, etc. (Yu et al. 2015).

Although the SAM variability and impacts thereof in the SO have been vastly studied over recent years, the impacts of said mode of variability at the regional-scale is less known, more specifically in the area south of the Subantarctic sector. As one of the primary drivers of wind circulation over the SO, if satellite and ground truthing observations all demonstrate increasing wind speeds over the SO, then this would suggest that the increase in SAM has a certain effect on wind speeds, and consequently the oceanography of the SO. Here, we discuss the influence of this leading mode of atmospheric variability on the SO using the results from the model analysis.

Steadily increasing measured wind speeds in the SO over the past few decades have coincided with identified positive trends in the SAM index (Manton et al. 2012). The SAM index describes the regional scale latitudinal movement of the westerly wind band in the SH. This north-south movement is broken into two phases with associated effects: a) positive and b) negative phase of SAM (Thompson and Solomon et al. 2007). We noted through correlation analysis that the positive phase of SAM index corresponds with significantly strengthening westerly winds in the AZ and southward towards Antarctica, and weakening westerly winds (easterly anomaly) in the SAZ and north towards the Equator (Figure 15). This shows the model SAM index - wind interaction is consistent with previous studies on the effects of SAM in the SO (Hartmann and Lo et al. 1998; Limpasuvan and Hartmann et al. 1999).

Our results show a positive correlation between the SAM index and mean MLD at the region between 55 - 60 °S and significant negative correlations northward and southward of the 55 - 60 °S (Figure 19). The negative correlations towards the poles can be attributed to the shift of westerly winds creating anomalies on poleward and equatorward Ekman transport in areas of negative correlations. This results in increased upwelling of cold, iron-enriched water into the AZ, the resulting response in the SAZ, is increased convergence and downwelling (Lovenduski and Gruber et al. 2005).

SO SST plays an important role in moderating the overall surface temperature of the Southern Hemisphere. Studies show that SST anomalies in the SO have seen a gradual decrease which has been linked to the strong global warming trends by several authors (Kostov et al. 2016 and references therein). Our results show a positive correlation between SAM index and mean SST equatorward of 55 °S and a negative correlation southward of 55 °S towards Antarctica. Several studies have suggested that the increase in SST at SAZ is an SST response to a poleward shift and strengthening of surface westerlies, which resembles positive phases of the SAM (Hall and Visbeck et al. 2002; Oke and England et al. 2004; Fyfe et al. 2007; Marshall et al. 2013; Purich et al. 2016). A positive SAM corresponds with anomalous northward Ekman transport in the high latitude regions of the Southern Hemisphere (Hall and Visbeck et al. 2002). This gives rise to surface cooling poleward of 55 °S and warming southward of 55 °S (Kostov et al. 2017; Lefebvre et al. 2004). However, ozone depletion and its consequences for ice coverage at the boundaries of Antarctica be intensifying the response of SST to SAM (Bitz and Polvani et al. 2012).

The strong circumpolar westerly winds that occur during positive SAM reduce meridional advection into Antarctica (Marshall et al. 2013). Also, the easterlies, resulting from both katabatic drainage and adjustment to large-scale horizontal pressure gradients (Parish and Bromwich et al. 2007), that dominates near-surface circulation in East Antarctic, are weakened in most regions around Antarctica. This reduces the turbulent flow of heat toward the surface of the ocean and hence leads to a reduction in surface potential temperature, resulting in a stronger surface inversion and cooler surface temperatures in areas of positive SAM (van den Broeke and van Lipzig et al. 2003; Marshall et al. 2013). SST correlations are in quantitative agreement with those from Hall and Visbeck (2002) and Lefebvre (2007).

Salinity is also relevant to biological processes, for example the life cycles of a number of organisms from phytoplankton to larger predators are affected by haline concentration and its variability (Beier et al. 2017). Our results in figure 17 show some anomalous positive correlations with the SAM index north of PF, followed by some negative correlations poleward of PF. The enhanced overturning during positive SAM and the increased northward currents SSS (Lefebvre et al. 2004)

Even though the influence of SAM on the sea-ice is not explored in this thesis, it is still important as it affects surface variables differently during phases of the SAM. For example, freshwater flux from sea ice melt affects salinity. The shift of the surface forcing towards the positive phase of SAM results in reduced mean sea ice concentration and thickness in the

SO, but increased ice covering area. In the Weddell Sea, the ice coverage is smaller, and the response of the sea ice-ocean system to the SAM is stronger than in other regions. These further reduce the salinity of surface and intermediate water, while deep water is more saline. The enhanced overturning and the increased currents to the north cause SSS to rise (Lefebvre et al. 2004).

The impact of the SAM on ocean mixed-layer depth, surface temperature, salinity and wind speed varies strongly for the different regions of the SO (Lefebvre et al. 2004). Signals at these different regions tend to cancel out, resulting in insignificant correlations between SAM and our metrics over the domain (Figure 19). Since correlations between SAM index and chosen variables are low in magnitude, changes in these variables may be as a result of another forcing influenced by the SAM. Using the example SAZ and AZ boxes (see Figure 6), the area surrounding the SAZ (between 30 - 50 °S) is associated with stronger winds, while the area encompassing AZ (between 50 - 70°S) is associated with weaker winds (Figure 15). This confirms our choices of box location (Section 2.2.3). The relationship between the SAM index and some of the ocean variables at the respective locations (SAZ and AZ) is weak and not significant. Yu et al. (2015) suggests that signals at these different regions tend to cancel out, resulting in insignificant correlations between the SAM and oceanography over the domain.

Correlations between SAM and frontal movement are rather low (Section 3.2.2). Shao et al. (2015) noted similar low correlations of SAF and PF with SAM (with higher correlations $r \leq \pm 0.6$), which they disregard due to “no coherent signal observed between SAM and fronts”. Suggesting that due to the lack of significant correlations, the position of fronts: SAF and PF may not necessarily be related to SAM but the bathymetry and methods used for frontal definition (Russell et al. 2013).

The effects of model resolution on the oceanography in the domain are examined by comparison between the high and low resolutions and in situ data from WOA13. Coarse-resolution and eddy-permitting models agree with observations giving similar large-scale distribution patterns. The model with higher resolution exhibits stronger frontal and feature definition, which is true for all metrics. The signal observed on the eddy-resolving model might be amplified by model sensitivity to the processes in the underlying ocean. This effect is noticeable in the correlation of frontal location with SAM (Sec. 3.2.2): while the eddy-permitting

model correlates more highly to the SAM/wind field changes, the eddy-resolving model shows high spatial variability in the response to SA. This may be because the eddy-permitting model can well resolve important processes on a larger-scale, however the model does not resolve mesoscale turbulence, hence the variability in the eddy-resolving model may be due to mesoscale eddies etc.

The effect of the SAM index on the underlying ocean processes also shows a temporal lag in seasonal peaks for the climatological cycles of SST and SSS for the two model resolutions (Sec. 3.1.3). For instance, SATLANTIC12 captures the signal of SST in the SO's AZ and SAZ earlier than SATLANTIC05, or vice versa. Whereas SSS signal is first captured by SATLANTIC05. Studies note that on longer timescales, a delayed response causes mesoscale eddy fields to intensify, resulting in enhanced poleward heat exchange which drives warming south of the PF (Stevens et al. 2008; Screen and Gillett, 2009). Additionally, the lag in SSS signal across models may be due to sea ice contributions. It is possible that SATLANTIC05 starts to freeze-up earlier and break up earlier. This lag may precondition the surface ocean thus favouring the deeper mixing in the SAZ. The strong seasonal cycle in the AZ is due to the annual melting of sea ice (Michel et al. 2007).

Similar to our results, Hallberg et al. (2006) found that even though model resolution does not affect the distribution pattern of these variables greatly, it does affect the response of the oceanic variables significantly. He further explains that the eddy-resolving model significantly affects both the structure of the overturning and its response to changes in wind stress. Our results show the eddy-resolving model (SATLANTIC12) to better represent the relationship between SAM and SO, producing patterns more similar to in situ data. Furthermore, a lag exists in capturing the response in the models: SATLANTIC12 captures the effects quicker.

4.1 Limitations

This work gives a first-order analysis and evaluation of two model configurations towards understanding the response of the surface ocean to the SAM. We recognize that the period of 10 years used for this analysis is too short to fully resolve long-term processes associated with large-scale events such as SAM, as they can take up to decades. The model output frequency (5 days) is also rather low to resolve short term changes. i.e. storms can form and dissipate in less than 5 days. This same methodology should be repeated on longer simulations with higher frequency output.

5. Conclusion

In this work, we have studied the response of the SO to the increase in the SAM index, as calculated by Marshall (2003), over 10 years using two model configurations: eddy-permitting and eddy-resolving SO models forced by ERA-Interim winds, and compared with the WOA13 in-situ data. It is shown that significant relationships exist between the SAM and oceanic variables: Wind speed, SSS, SST and MLD over the SO. Furthermore, the models show similar response patterns when respective oceanic variables are correlated with the SAM, with a few notable differences between the models. An inter-comparison models: between SATLANTIC05 and across the SATLANTIC12 shows similar trends for the variables analysed with a temporal lag between the models.

The increase in greenhouse gasses and ozone depletion induced by human activity has been shown to contribute to the upward trend of the SAM, which is expected to continue in the future (Treguier et al. 2010). This increase in SAM can either strengthen or weaken the influence of the SAM over the SO. However, these influences of SAM are not fully understood, hence a ‘better’ representation of the ocean’s response to SAM is crucial.

References

Anderson, D.L.T. and Balmaseda, M., 2005. Overview of ocean models at ECMWF. In Proc. Seminar on Recent Developments in Numerical Methods for Atmospheric and Ocean Modelling (pp. 103-111).

Anderson, R.F., Ali, S., Bradtmiller, L.I., Nielsen, S.H.H., Fleisher, M.Q., Anderson, B.E. and Burckle, L.H., 2009. Wind-driven upwelling in the Southern Ocean and the deglacial rise in atmospheric CO2. Science, 323(5920), pp.1443-1448.

Athanase, M., Sennéchael, N., Garric, G., Koenig, Z., Boles, E. and Provost, C., 2019. New Hydrographic Measurements of the Upper Arctic Western Eurasian Basin in 2017 Reveal Fresher Mixed Layer and Shallower Warm Layer Than 2005–2012 Climatology. Journal of Geophysical Research: Oceans, 124(2), pp.1091-1114.

Arrigo, K.R., van Dijken, G.L. and Bushinsky, S., 2008. Primary production in the Southern Ocean, 1997–2006. Journal of Geophysical Research: Oceans, 113(C8).

Beier, E., Bernal, G., Ruiz-Ochoa, M. and Barton, E.D., 2017. Freshwater exchanges and surface salinity in the Colombian basin, Caribbean Sea. PloS one, 12(8), p.e0182116.

Bitz, C.M. and Polvani, L.M., 2012. Antarctic climate response to stratospheric ozone depletion in a fine resolution ocean climate model. Geophysical Research Letters, 39(20).

Bracegirdle, T.J. and Marshall, G.J., 2012. The reliability of Antarctic tropospheric pressure and temperature in the latest global reanalyses. Journal of Climate, 25(20), pp.7138-7146.

Bulusu, S. and Ferster, B., 2017, September. Investigating the role of the Southern Ocean on global climate change. In OCEANS 2017-Anchorage (pp. 1-4). IEEE.

Chaigneau, A. and Morrow, R., 2002. Surface temperature and salinity variations between Tasmania and Antarctica, 1993–1999. Journal of Geophysical Research: Oceans, 107(C12).

Cori, A., Ayles, H., Beyers, N., Schaap, A., Floyd, S., Sabapathy, K., Eaton, J.W., Hauck, K., Smith, P., Griffith, S. and Moore, A., 2014. HPTN 071 (PopART): a cluster-randomized trial of the population impact of an HIV combination prevention intervention including universal testing and treatment: mathematical model. PloS one, 9(1), p.e84511.

Davies, Bethan, and Bethan Davies. “Changes to Circumpolar Deep Water.” AntarcticGlaciers.org. Accessed 17, 2019. http://www.antarcticglaciers.org/glaciers-and-climate/ice-ocean-interactions/changes-circumpolar-deep-water/.

de Boyer Montégut, C., Madec, G., Fischer, A. S., Lazar, A., & Iudicone, D. (2004). Mixed layer depth over the global ocean: An examination of profile data and a profile-based climatology. Journal of Geophysical Research: Oceans, 109(C12).

Dee, D.P., Uppala, S.M., Simmons, A.J., Berrisford, P., Poli, P., Kobayashi, S., Andrae, U., Balmaseda, M.A., Balsamo, G., Bauer, D.P. and Bechtold, P., 2011. The ERA-Interim reanalysis: Configuration and performance of the data assimilation system. Quarterly Journal of the Royal Meteorological Society, 137(656), pp.553-597.

Deppeler, S.L. and Davidson, A.T., 2017. Southern Ocean phytoplankton in a changing climate. Frontiers in Marine Science, 4, p.40.

Dinniman, M.S., Klinck, J.M. and Hofmann, E.E., 2012. Sensitivity of Circumpolar Deep Water transport and ice shelf basal melt along the west Antarctic Peninsula to changes in the winds. Journal of Climate, 25(14), pp.4799-4816.

Farneti, R. and Delworth, T.L., 2010. The role of mesoscale eddies in the remote oceanic response to altered Southern Hemisphere winds. Journal of Physical Oceanography, 40(10), pp.2348-2354.

Fogt, R.L., Bromwich, D.H. and Hines, K.M., 2011. Understanding the SAM influence on the South Pacific ENSO teleconnection. Climate Dynamics, 36(7-8), pp.1555-1576.

Gillett, N.P., Kell, T.D. and Jones, P.D., 2006. Regional climate impacts of the Southern Annular Mode. Geophysical Research Letters, 33(23).

Griffies, S., 2018. Fundamentals of ocean climate models. Princeton University press.

Gruber, N., Landschützer, P. and Lovenduski, N.S., 2019. The variable Southern Ocean carbon sink. Annual review of marine science, 11, pp.159-186.

Hande, L.B., Siems, S.T. and Manton, M.J., 2012. Observed trends in wind speed over the Southern Ocean. Geophysical Research Letters, 39(11).

Hartin, C.A., Fine, R.A., Sloyan, B.M., Talley, L.D., Chereskin, T.K. and Happell, J., 2011. Formation rates of Subantarctic mode water and Antarctic intermediate water within the South Pacific. Deep Sea Research Part I: Oceanographic Research Papers, 58(5), pp.524-534.

Hartmann, D.L. and Lo, F., 1998. Wave-driven zonal flow vacillation in the Southern Hemisphere. Journal of the Atmospheric Sciences, 55(8), pp.1303-1315.

Hauck, J., Völker, C., Wang, T., Hoppema, M., Losch, M. and Wolf-Gladrow, D.A., 2013. Seasonally different carbon flux changes in the Southern Ocean in response to the southern annular mode. Global Biogeochemical Cycles, 27(4), pp.1236-1245.

Hernández, A.S.R., Trull, T.W., Nodder, S.D. and Flores, J.A., 2019. Coccolithophore biodiversity controls carbonate export in the Southern Ocean.

Ho, M., Kiem, A.S. and Verdon-Kidd, D.C., 2012. The Southern Annular Mode: a comparison of indices. Hydrology and Earth System Sciences, 16(3), pp.967-982.

Holte, J., Talley, L.D., Gilson, J. and Roemmich, D., 2017. An Argo mixed layer climatology and database. Geophysical Research Letters, 44(11), pp.5618-5626.

Hu, A., Meehl, G., Stammer, D., Han, W. and Strand, W., 2017. Role of perturbing ocean initial conditions in simulated regional sea level change. Water, 9(6), p.401.

Jaeger, A., Jaquemet, S., Phillips, R.A., Wanless, R.M., Richard, P. and Cherel, Y., 2013. Stable isotopes document inter-and intra-specific variation in feeding ecology of nine large southern Procellariiformes. Marine Ecology Progress Series, 490, pp.255-266.

Kara, A.B., Rochford, P.A. and Hurlburt, H.E., 2003. Mixed layer depth variability over the global ocean. Journal of Geophysical Research: Oceans, 108(C3).

Kidston, J., Renwick, J.A. and McGregor, J., 2009. Hemispheric-scale seasonality of the Southern Annular Mode and impacts on the climate of New Zealand. Journal of Climate, 22(18), pp.4759-4770.

Kostov, Y., Marshall, J., Hausmann, U., Armour, K.C., Ferreira, D. and Holland, M.M., 2017. Fast and slow responses of Southern Ocean sea surface temperature to SAM in coupled climate models. Climate Dynamics, 48(5-6), pp.1595-1609.

Lévy, M., Estublier, A. and Madec, G., 2001. Choice of an advection scheme for biogeochemical models. Geophysical Research Letters, 28(19), pp.3725-3728.

Limpasuvan, V. and Hartmann, D.L., 1999. Eddies and the annular modes of climate variability. Geophysical Research Letters, 26(20), pp.3133-3136.

Lovenduski, N.S. and Gruber, N., 2005. Impact of the Southern Annular Mode on Southern Ocean circulation and biology. Geophysical Research Letters, 32(11).

Madec, G. and Imbard, M., 1996. A global ocean mesh to overcome the North Pole singularity. Climate Dynamics, 12(6), pp.381-388.

Manucharyan, G.E. and Thompson, A.F., 2017. Submesoscale sea ice-ocean interactions in marginal ice zones. Journal of Geophysical Research: Oceans, 122(12), pp.9455-9475.

Marshall, G.J., Orr, A. and Turner, J., 2013. A predominant reversal in the relationship between the SAM and East Antarctic temperatures during the twenty-first century. Journal of Climate, 26(14), pp.5196-5204.

Marshall, G., & National Center for Atmospheric Research Staff (Eds). Last modified 19 Mar 2018. "The Climate Data Guide: Marshall Southern Annular Mode (SAM) Index (Station-based)." Retrieved from https://climatedataguide.ucar.edu/climate-data/marshall-southern-annular-mode-sam-index-station-based.

Parker, Wendy, "Climate Science", The Stanford Encyclopedia of Philosophy (Summer 2018 Edition), Edward N. Zalta (ed.), URL = <https://plato.stanford.edu/archives/sum2018/entries/climate-science/>.

Purich, A., Cai, W., England, M.H. and Cowan, T., 2016. Evidence for link between modelled trends in Antarctic sea ice and underestimated westerly wind changes. Nature communications, 7, p.10409.

Rintoul, S.R., Hughes, C.W. and Olbers, D., 2001. .6 The t system. In International Geophysics (Vol. 77, pp. 271-XXXVI). Academic Press.

Rintoul, S.R. and Garabato, A.C.N., 2013. Dynamics of the Southern Ocean circulation. In International Geophysics (Vol. 103, pp. 471-492). Academic Press.

Russell, J.L., Kamenkovich, I., Bitz, C., Ferrari, R., Gille, S.T., Goodman, P.J., Hallberg, R., Johnson, K., Khazmutdinova, K., Marinov, I. and Mazloff, M., 2018. Metrics for the evaluation of the Southern Ocean in coupled climate models and earth system models. Journal of Geophysical Research: Oceans, 123(5), pp.3120-3143.

Sarmiento, J.L., Gruber, N., Brzezinski, M.A. and Dunne, J.P., 2004. High-latitude controls of thermocline nutrients and low latitude biological productivity. Nature, 427(6969), p.56.

Schmittner, A., Chiang, J.C. and Hemming, S.R., 2007. Introduction: The ocean's meridional overturning circulation. Washington DC American Geophysical Union Geophysical.

Madec, G., and NEMO System Team. 2015. NEMO ocean engine. NEMO Consortium, edition. doi:10.5281/zenodo.1464816. Monograph Series, 173, pp.1-4.

Schmittner, A., Chiang, J.C. and Hemming, S.R., 2007. Introduction: The ocean's meridional overturning circulation. Washington DC American Geophysical Union Geophysical Monograph Series, 173, pp.1-4.

Screen, J.A., Gillett, N.P., Stevens, D.P., Marshall, G.J. and Roscoe, H.K., 2009. The role of eddies in the Southern Ocean temperature response to the Southern Annular Mode. Journal of Climate, 22(3), pp.806-818.

Shao, A.E., Gille, S.T., Mecking, S. and Thompson, L., 2015. Properties of the Subantarctic Front and Polar Front from the skewness of sea level anomaly. Journal of Geophysical Research: Oceans, 120(7), pp.5179-5193.

Sloyan, B.M. and Rintoul, S.R., 2001. The Southern Ocean limb of the global deep overturning circulation. Journal of Physical Oceanography, 31(1), pp.143-173.

Spence, P., Fyfe, J.C., Montenegro, A. and Weaver, A.J., 2010. Southern Ocean response to strengthening winds in an eddy-permitting global climate model. Journal of Climate, 23(19), pp.5332-5343.

Steele, J.H., Thorpe, S.A. and Turekian, K.K. eds., 2009. Elements of physical oceanography: a derivative of the encyclopedia of ocean sciences. Academic Press, pp. 231

Swart, N.C., Gille, S.T., Fyfe, J.C. and Gillett, N.P., 2018. Recent Southern Ocean warming and freshening driven by greenhouse gas emissions and ozone depletion. Nature Geoscience, 11(11), p.836.

Swart, S., Chang, N., Fauchereau, N., Joubert, W., Lucas, M., Mtshali, T., Roychoudhury, A., Tagliabue, A., Thomalla, S., Waldron, H. and Monteiro, P., 2012. Southern Ocean Seasonal Cycle Experiment 2012: Seasonal scale climate and carbon cycle links. South African Journal of Science, 108(3-4), pp.11-13.

Tetzner, D., Thomas, E. and Allen, C., 2019. A Validation of ERA5 Reanalysis Data in the Southern Antarctic Peninsula—Ellsworth Land Region, and Its Implications for Ice Core Studies. Geosciences, 9(7), p.289.

Thomalla, S.J., Fauchereau, N., Swart, S. and Monteiro, P.M.S., 2011. Regional scale characteristics of the seasonal cycle of chlorophyll in the Southern Ocean. Biogeosciences, 8(10), pp.2849-2866.

Thompson, D.W. and Solomon, S., 2002. Interpretation of recent Southern Hemisphere climate change. Science, 296(5569), pp.895-899.

Tréguier, A.M., Le Sommer, J., Molines, J.M. and De Cuevas, B., 2010. Response of the Southern Ocean to the Southern Annular Mode: Interannual variability and multidecadal trend. Journal of Physical Oceanography, 40(7), pp.1659-1668.

Trull, T.W., Sedwick, P.N., Griffiths, F.B. and Rintoul, S.R., 2001. Introduction to special section: SAZ Project. Journal of Geophysical Research: Oceans, 106(C12), pp.31425-31429.

Van Den Broeke, M.R. and Van Lipzig, N.P., 2004. Changes in Antarctic temperature, wind and precipitation in response to the Antarctic Oscillation. Annals of Glaciology, 39, pp.119-126.

Wolf C. Protist diversity and biogeography in the Pacific sector of the Southern Ocean (Doctoral dissertation, Jacobs University Bremen).

Yu, J.Y., Paek, H., Saltzman, E.S. and Lee, T., 2015. The early 1990s change in ENSO–PSA–SAM relationships and its impact on Southern Hemisphere climate. Journal of Climate, 28(23), pp.9393-9408.

Bibliography

Anderson, D.L.T. and Balmaseda, M., 2005. Overview of ocean models at ECMWF. In Proc. Seminar on Recent Developments in Numerical Methods for Atmospheric and Ocean Modelling (pp. 103-111).

Anderson, R.F., Ali, S., Bradtmiller, L.I., Nielsen, S.H.H., Fleisher, M.Q., Anderson, B.E. and Burckle, L.H., 2009. Wind-driven upwelling in the Southern Ocean and the deglacial rise in atmospheric CO2. Science, 323(5920), pp.1443-1448.

Athanase, M., Sennéchael, N., Garric, G., Koenig, Z., Boles, E. and Provost, C., 2019. New Hydrographic Measurements of the Upper Arctic Western Eurasian Basin in 2017 Reveal Fresher Mixed Layer and Shallower Warm Layer Than 2005–2012 Climatology. Journal of Geophysical Research: Oceans, 124(2), pp.1091-1114.

Arrigo, K.R., van Dijken, G.L. and Bushinsky, S., 2008. Primary production in the Southern Ocean, 1997–2006. Journal of Geophysical Research: Oceans, 113(C8).

Beier, E., Bernal, G., Ruiz-Ochoa, M. and Barton, E.D., 2017. Freshwater exchanges and surface salinity in the Colombian basin, Caribbean Sea. PloS one, 12(8), p.e0182116.

Bitz, C.M. and Polvani, L.M., 2012. Antarctic climate response to stratospheric ozone depletion in a fine resolution ocean climate model. Geophysical Research Letters, 39(20).

Bracegirdle, T.J. and Marshall, G.J., 2012. The reliability of Antarctic tropospheric pressure and temperature in the latest global reanalyses. Journal of Climate, 25(20), pp.7138-7146.

Bulusu, S. and Ferster, B., 2017, September. Investigating the role of the Southern Ocean on global climate change. In OCEANS 2017-Anchorage (pp. 1-4). IEEE.

Chaigneau, A. and Morrow, R., 2002. Surface temperature and salinity variations between Tasmania and Antarctica, 1993–1999. Journal of Geophysical Research: Oceans, 107(C12).

Cori, A., Ayles, H., Beyers, N., Schaap, A., Floyd, S., Sabapathy, K., Eaton, J.W., Hauck, K., Smith, P., Griffith, S. and Moore, A., 2014. HPTN 071 (PopART): a cluster-randomized trial of the population impact of an HIV combination prevention intervention including universal testing and treatment: mathematical model. PloS one, 9(1), p.e84511.

Davies, Bethan, and Bethan Davies. “Changes to Circumpolar Deep Water.” AntarcticGlaciers.org. Accessed 17, 2019. http://www.antarcticglaciers.org/glaciers-and-climate/ice-ocean-interactions/changes-circumpolar-deep-water/.

de Boyer Montégut, C., Madec, G., Fischer, A. S., Lazar, A., & Iudicone, D. (2004). Mixed layer depth over the global ocean: An examination of profile data and a profile-based climatology. Journal of Geophysical Research: Oceans, 109(C12).

Dee, D.P., Uppala, S.M., Simmons, A.J., Berrisford, P., Poli, P., Kobayashi, S., Andrae, U., Balmaseda, M.A., Balsamo, G., Bauer, D.P. and Bechtold, P., 2011. The ERA-Interim reanalysis: Configuration and performance of the data assimilation system. Quarterly Journal of the Royal Meteorological Society, 137(656), pp.553-597.

Deppeler, S.L. and Davidson, A.T., 2017. Southern Ocean phytoplankton in a changing climate. Frontiers in Marine Science, 4, p.40.

Dinniman, M.S., Klinck, J.M. and Hofmann, E.E., 2012. Sensitivity of Circumpolar Deep Water transport and ice shelf basal melt along the west Antarctic Peninsula to changes in the winds. Journal of Climate, 25(14), pp.4799-4816.

Farneti, R. and Delworth, T.L., 2010. The role of mesoscale eddies in the remote oceanic response to altered Southern Hemisphere winds. Journal of Physical Oceanography, 40(10), pp.2348-2354.

Fogt, R.L., Bromwich, D.H. and Hines, K.M., 2011. Understanding the SAM influence on the South Pacific ENSO teleconnection. Climate Dynamics, 36(7-8), pp.1555-1576.

Gillett, N.P., Kell, T.D. and Jones, P.D., 2006. Regional climate impacts of the Southern Annular Mode. Geophysical Research Letters, 33(23).

Griffies, S., 2018. Fundamentals of ocean climate models. Princeton University press.

Gruber, N., Landschützer, P. and Lovenduski, N.S., 2019. The variable Southern Ocean carbon sink. Annual review of marine science, 11, pp.159-186.

Hande, L.B., Siems, S.T. and Manton, M.J., 2012. Observed trends in wind speed over the Southern Ocean. Geophysical Research Letters, 39(11).

Hartin, C.A., Fine, R.A., Sloyan, B.M., Talley, L.D., Chereskin, T.K. and Happell, J., 2011. Formation rates of Subantarctic mode water and Antarctic intermediate water within the South Pacific. Deep Sea Research Part I: Oceanographic Research Papers, 58(5), pp.524-534.

Hartmann, D.L. and Lo, F., 1998. Wave-driven zonal flow vacillation in the Southern Hemisphere. Journal of the Atmospheric Sciences, 55(8), pp.1303-1315.

Hauck, J., Völker, C., Wang, T., Hoppema, M., Losch, M. and Wolf-Gladrow, D.A., 2013. Seasonally different carbon flux changes in the Southern Ocean in response to the southern annular mode. Global Biogeochemical Cycles, 27(4), pp.1236-1245.

Hernández, A.S.R., Trull, T.W., Nodder, S.D. and Flores, J.A., 2019. Coccolithophore biodiversity controls carbonate export in the Southern Ocean.

Ho, M., Kiem, A.S. and Verdon-Kidd, D.C., 2012. The Southern Annular Mode: a comparison of indices. Hydrology and Earth System Sciences, 16(3), pp.967-982.

Holte, J., Talley, L.D., Gilson, J. and Roemmich, D., 2017. An Argo mixed layer climatology and database. Geophysical Research Letters, 44(11), pp.5618-5626.

Hu, A., Meehl, G., Stammer, D., Han, W. and Strand, W., 2017. Role of perturbing ocean initial conditions in simulated regional sea level change. Water, 9(6), p.401.

Jaeger, A., Jaquemet, S., Phillips, R.A., Wanless, R.M., Richard, P. and Cherel, Y., 2013. Stable isotopes document inter-and intra-specific variation in feeding ecology of nine large southern Procellariiformes. Marine Ecology Progress Series, 490, pp.255-266.

Kara, A.B., Rochford, P.A. and Hurlburt, H.E., 2003. Mixed layer depth variability over the global ocean. Journal of Geophysical Research: Oceans, 108(C3).

Kidston, J., Renwick, J.A. and McGregor, J., 2009. Hemispheric-scale seasonality of the Southern Annular Mode and impacts on the climate of New Zealand. Journal of Climate, 22(18), pp.4759-4770.

Kostov, Y., Marshall, J., Hausmann, U., Armour, K.C., Ferreira, D. and Holland, M.M., 2017. Fast and slow responses of Southern Ocean sea surface temperature to SAM in coupled climate models. Climate Dynamics, 48(5-6), pp.1595-1609.

Lévy, M., Estublier, A. and Madec, G., 2001. Choice of an advection scheme for biogeochemical models. Geophysical Research Letters, 28(19), pp.3725-3728.

Limpasuvan, V. and Hartmann, D.L., 1999. Eddies and the annular modes of climate variability. Geophysical Research Letters, 26(20), pp.3133-3136.

Lovenduski, N.S. and Gruber, N., 2005. Impact of the Southern Annular Mode on Southern Ocean circulation and biology. Geophysical Research Letters, 32(11).

Madec, G. and Imbard, M., 1996. A global ocean mesh to overcome the North Pole singularity. Climate Dynamics, 12(6), pp.381-388.

Manucharyan, G.E. and Thompson, A.F., 2017. Submesoscale sea ice-ocean interactions in marginal ice zones. Journal of Geophysical Research: Oceans, 122(12), pp.9455-9475.

Marshall, G.J., Orr, A. and Turner, J., 2013. A predominant reversal in the relationship between the SAM and East Antarctic temperatures during the twenty-first century. Journal of Climate, 26(14), pp.5196-5204.

Marshall, G., & National Center for Atmospheric Research Staff (Eds). Last modified 19 Mar 2018. "The Climate Data Guide: Marshall Southern Annular Mode (SAM) Index (Station-based)." Retrieved from https://climatedataguide.ucar.edu/climate-data/marshall-southern-annular-mode-sam-index-station-based.

Parker, Wendy, "Climate Science", The Stanford Encyclopedia of Philosophy (Summer 2018 Edition), Edward N. Zalta (ed.), URL = <https://plato.stanford.edu/archives/sum2018/entries/climate-science/>.

Purich, A., Cai, W., England, M.H. and Cowan, T., 2016. Evidence for link between modelled trends in Antarctic sea ice and underestimated westerly wind changes. Nature communications, 7, p.10409.

Rintoul, S.R., Hughes, C.W. and Olbers, D., 2001. .6 The t system. In International Geophysics (Vol. 77, pp. 271-XXXVI). Academic Press.

Rintoul, S.R. and Garabato, A.C.N., 2013. Dynamics of the Southern Ocean circulation. In International Geophysics (Vol. 103, pp. 471-492). Academic Press.

Russell, J.L., Kamenkovich, I., Bitz, C., Ferrari, R., Gille, S.T., Goodman, P.J., Hallberg, R., Johnson, K., Khazmutdinova, K., Marinov, I. and Mazloff, M., 2018. Metrics for the evaluation of the Southern Ocean in coupled climate models and earth system models. Journal of Geophysical Research: Oceans, 123(5), pp.3120-3143.

Sarmiento, J.L., Gruber, N., Brzezinski, M.A. and Dunne, J.P., 2004. High-latitude controls of thermocline nutrients and low latitude biological productivity. Nature, 427(6969), p.56.

Schmittner, A., Chiang, J.C. and Hemming, S.R., 2007. Introduction: The ocean's meridional overturning circulation. Washington DC American Geophysical Union Geophysical.

Madec, G., and NEMO System Team. 2015. NEMO ocean engine. NEMO Consortium, edition. doi:10.5281/zenodo.1464816. Monograph Series, 173, pp.1-4.

Schmittner, A., Chiang, J.C. and Hemming, S.R., 2007. Introduction: The ocean's meridional overturning circulation. Washington DC American Geophysical Union Geophysical Monograph Series, 173, pp.1-4.

Screen, J.A., Gillett, N.P., Stevens, D.P., Marshall, G.J. and Roscoe, H.K., 2009. The role of eddies in the Southern Ocean temperature response to the Southern Annular Mode. Journal of Climate, 22(3), pp.806-818.

Shao, A.E., Gille, S.T., Mecking, S. and Thompson, L., 2015. Properties of the Subantarctic Front and Polar Front from the skewness of sea level anomaly. Journal of Geophysical Research: Oceans, 120(7), pp.5179-5193.

Sloyan, B.M. and Rintoul, S.R., 2001. The Southern Ocean limb of the global deep overturning circulation. Journal of Physical Oceanography, 31(1), pp.143-173.

Spence, P., Fyfe, J.C., Montenegro, A. and Weaver, A.J., 2010. Southern Ocean response to strengthening winds in an eddy-permitting global climate model. Journal of Climate, 23(19), pp.5332-5343.

Steele, J.H., Thorpe, S.A. and Turekian, K.K. eds., 2009. Elements of physical oceanography: a derivative of the encyclopedia of ocean sciences. Academic Press, pp. 231

Swart, N.C., Gille, S.T., Fyfe, J.C. and Gillett, N.P., 2018. Recent Southern Ocean warming and freshening driven by greenhouse gas emissions and ozone depletion. Nature Geoscience, 11(11), p.836.

Swart, S., Chang, N., Fauchereau, N., Joubert, W., Lucas, M., Mtshali, T., Roychoudhury, A., Tagliabue, A., Thomalla, S., Waldron, H. and Monteiro, P., 2012. Southern Ocean Seasonal Cycle Experiment 2012: Seasonal scale climate and carbon cycle links. South African Journal of Science, 108(3-4), pp.11-13.

Tetzner, D., Thomas, E. and Allen, C., 2019. A Validation of ERA5 Reanalysis Data in the Southern Antarctic Peninsula—Ellsworth Land Region, and Its Implications for Ice Core Studies. Geosciences, 9(7), p.289.

Thomalla, S.J., Fauchereau, N., Swart, S. and Monteiro, P.M.S., 2011. Regional scale characteristics of the seasonal cycle of chlorophyll in the Southern Ocean. Biogeosciences, 8(10), pp.2849-2866.

Thompson, D.W. and Solomon, S., 2002. Interpretation of recent Southern Hemisphere climate change. Science, 296(5569), pp.895-899.

Tréguier, A.M., Le Sommer, J., Molines, J.M. and De Cuevas, B., 2010. Response of the Southern Ocean to the Southern Annular Mode: Interannual variability and multidecadal trend. Journal of Physical Oceanography, 40(7), pp.1659-1668.

Trull, T.W., Sedwick, P.N., Griffiths, F.B. and Rintoul, S.R., 2001. Introduction to special section: SAZ Project. Journal of Geophysical Research: Oceans, 106(C12), pp.31425-31429.

Van Den Broeke, M.R. and Van Lipzig, N.P., 2004. Changes in Antarctic temperature, wind and precipitation in response to the Antarctic Oscillation. Annals of Glaciology, 39, pp.119-126.

Wolf C. Protist diversity and biogeography in the Pacific sector of the Southern Ocean (Doctoral dissertation, Jacobs University Bremen).

Yu, J.Y., Paek, H., Saltzman, E.S. and Lee, T., 2015. The early 1990s change in ENSO–PSA–SAM relationships and its impact on Southern Hemisphere climate. Journal of Climate, 28(23), pp.9393-9408.